Light DM Search with NV Centers in Diamonds

SC, M. Hazumi, D. Herbschleb, N. Mizuochi, K. Nakayama

arXiv: 2302.12756

BERKELEY LAB

International Center for Quantum-field Measurement Systems for Studies of the Universe and Particles
WPI research center at KEK

So Chigusa

11/13/2023 @ UC Davis

Dark Matter as a hint of new physics

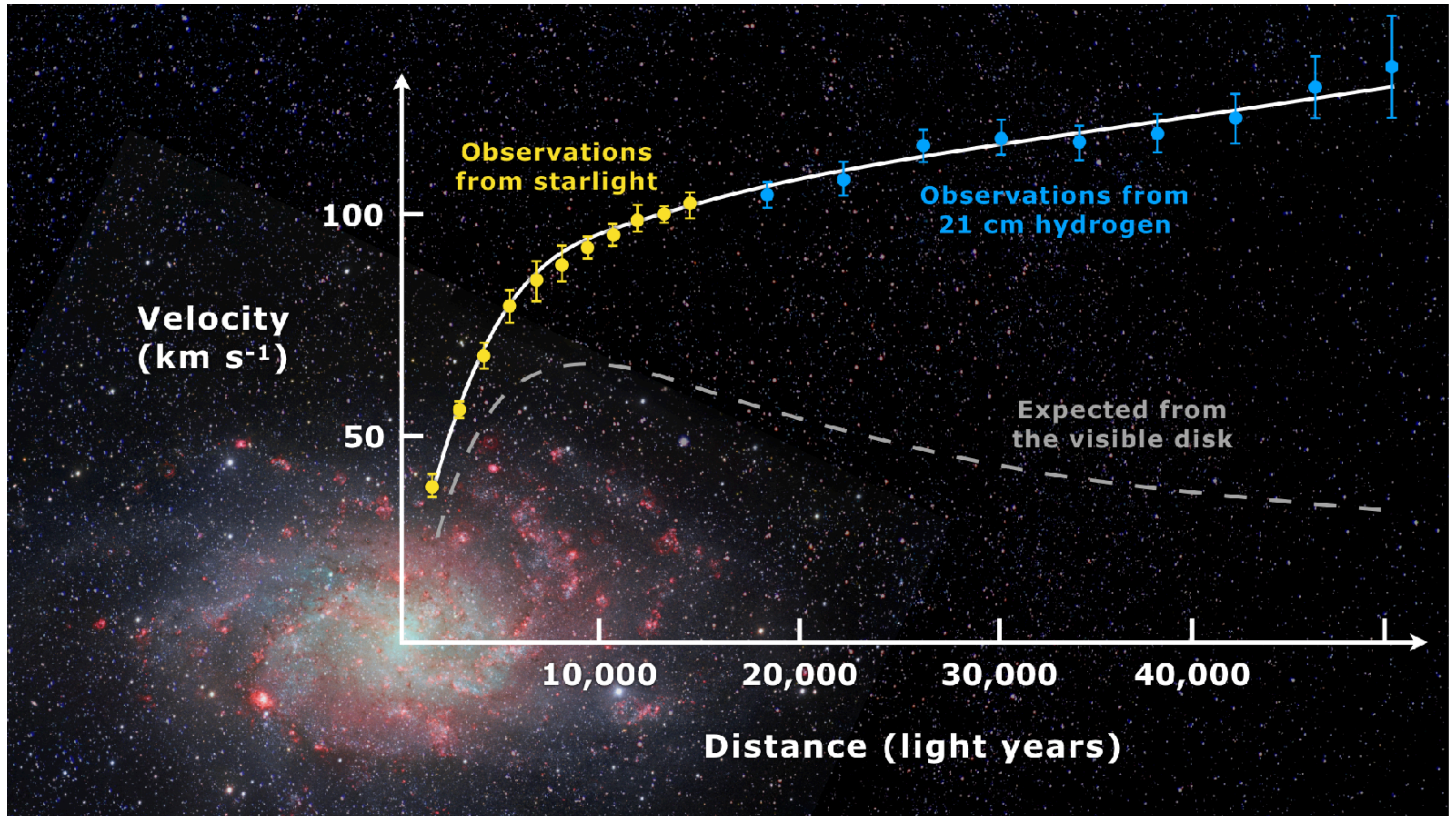

Wikipedia "Galaxy rotation curve", E. Corbelli, P. Salucci (2000)

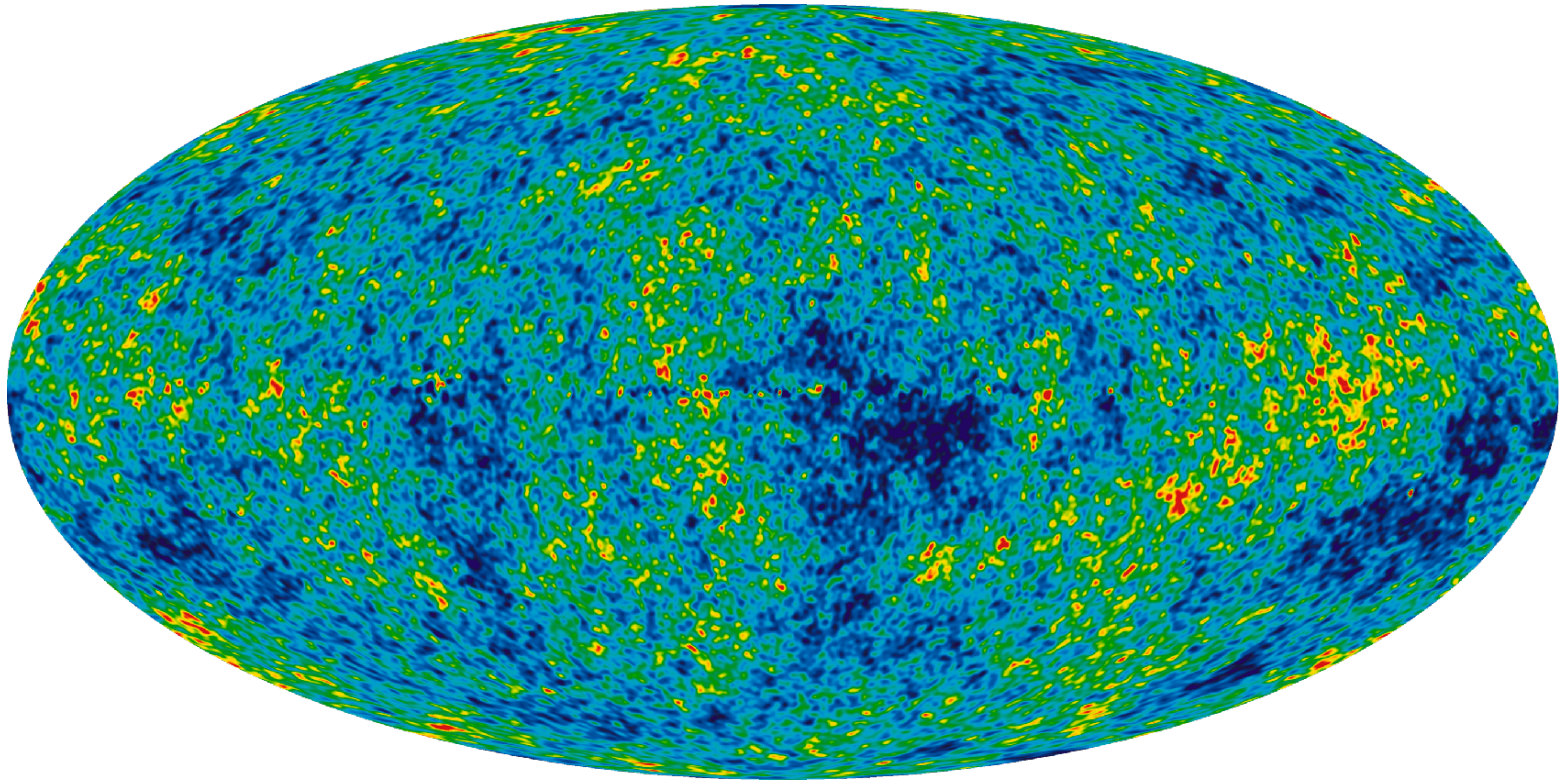

Wikipedia "Cosmic microwave background", 9 years of WMAP data

"Known"

✓ DM existence, abundance
✓ Has gravitational interaction

"Unknown"

✓ DM mass
✓ Non-gravitational interactions

DM mass window

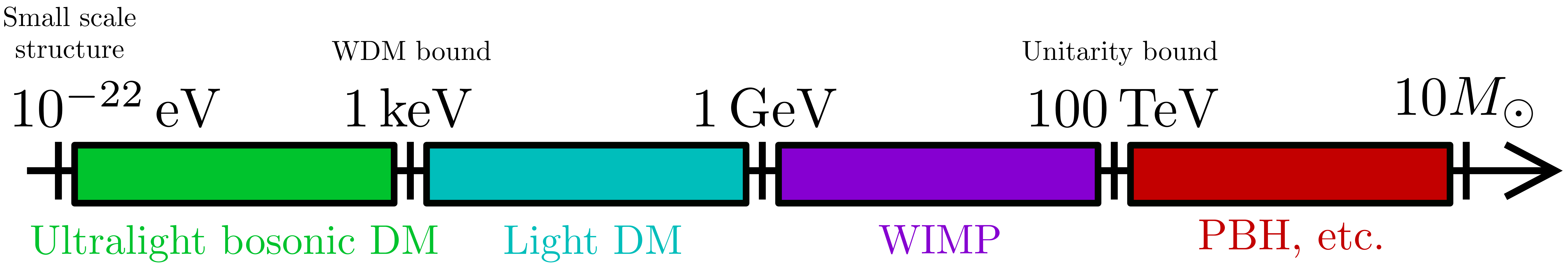

- WIMP miracle w/ thermal production of $\mathcal{O}(1)\,\mathrm{TeV}$
- Other interaction and production mechanisms allow a broader mass range
  - freeze-in
  - misalignment mechanism for light bosonic DM ⟵

Nelson+ '11, Arias+ '12

Light bosonic DM

- QCD axion
- Axion-like particles (ALPs)

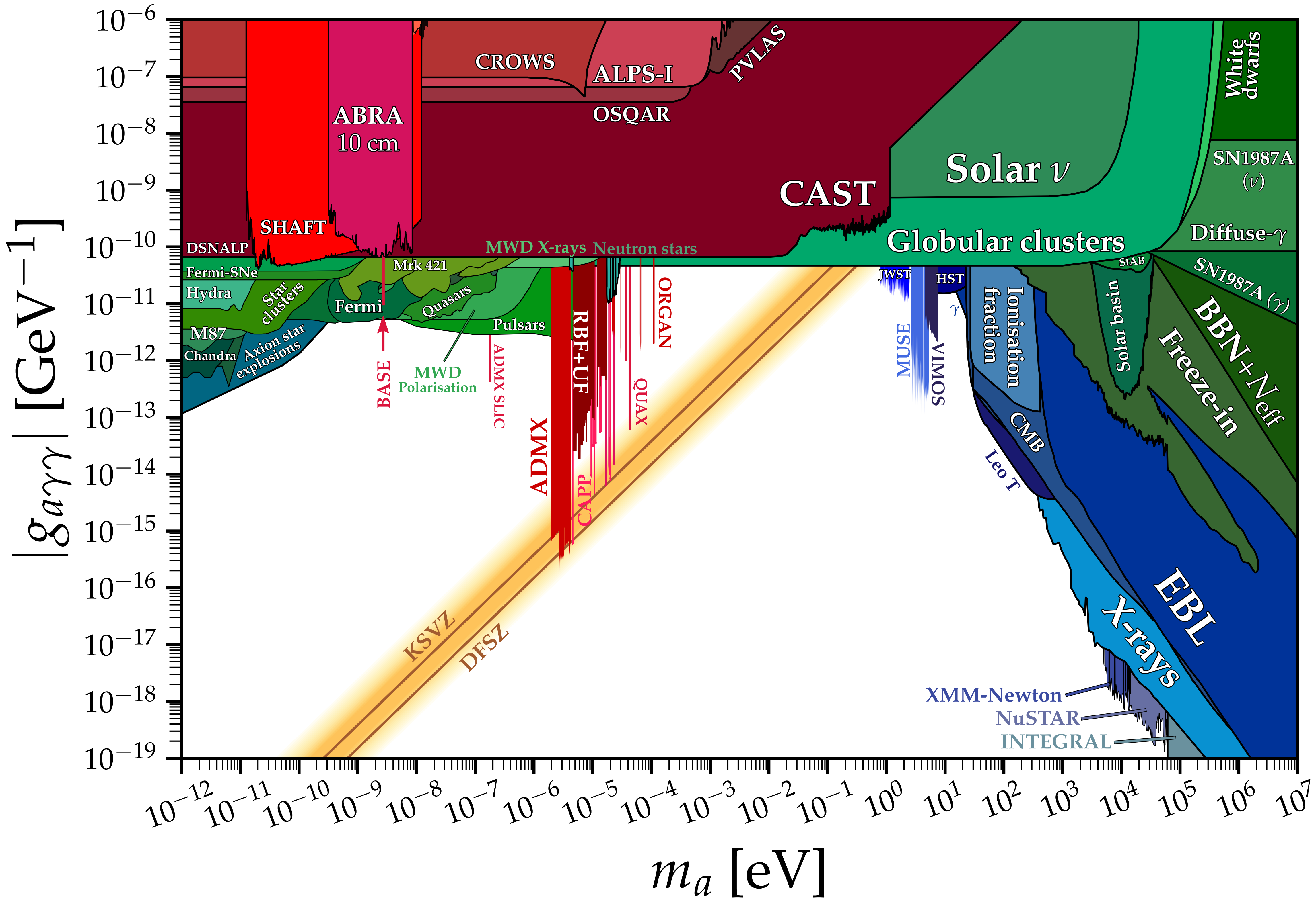

- Dark photon

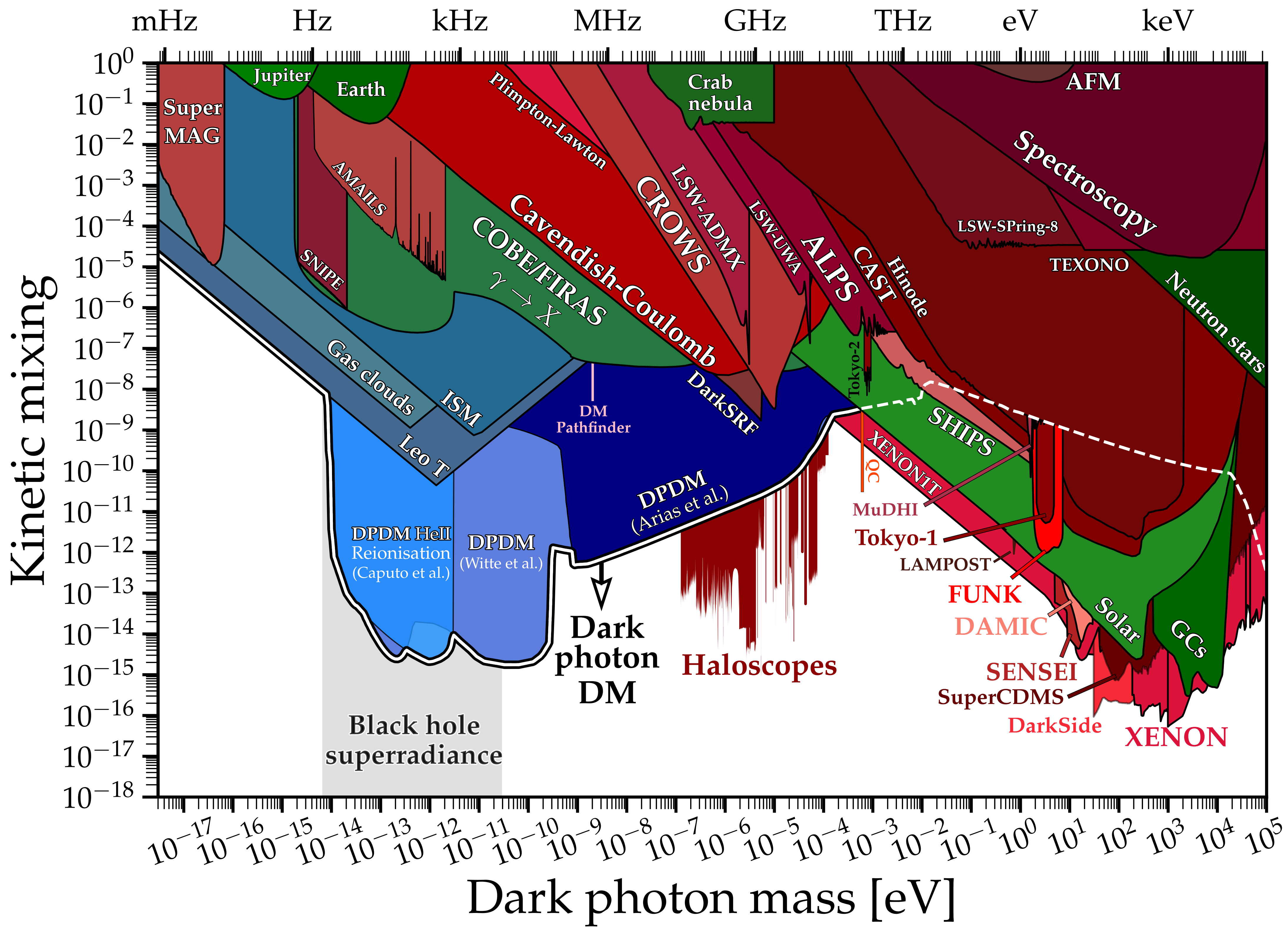

O'Hare "AxionLimits"

DM-induced electromagnetic field

- QCD axion / axion-like particles (ALPs)

$$\mathscr{L} = g_{aff}\frac{\partial_\mu a}{2m_f}\bar{f}\gamma^\mu\gamma_5 f \;\rightarrow\; H_{\rm eff} = \frac{g_{aff}}{m_f}\nabla a\cdot\mathbf{S}_f$$

$$\mathbf{B}_{\rm eff} \simeq \sqrt{2\rho_{\rm DM}}\,\frac{g_{aff}}{e}\mathbf{v}_{\rm DM}\cos(mt+\delta) \sim 3\,\mathrm{aT}\left(\frac{g_{aff}}{10^{-10}}\right)$$

- Dark photon

$$\mathbf{B}_{\rm eff} = \sqrt{2\rho_{\rm DM}}\,\epsilon\left(\mathbf{v}_{\rm DM}\times\hat{H}\right)\cos(mt+\delta) \sim 1\,\mathrm{aT}\left(\frac{\epsilon}{10^{-10}}\right)$$

- Behaves as an effective EM field with coherence time

$$\tau_{\rm DM} = \frac{2\pi}{m_{\rm DM}v_{\rm DM}^2} \sim 6s\left(\frac{10^{-10}\,\mathrm{eV}}{m_{\rm DM}}\right)$$

$$a(t) \simeq a_0\cos\left(m_a t + \frac{1}{2}m_a v_a^2 t - \vec{v}_a\cdot\vec{x} + \delta\right)$$

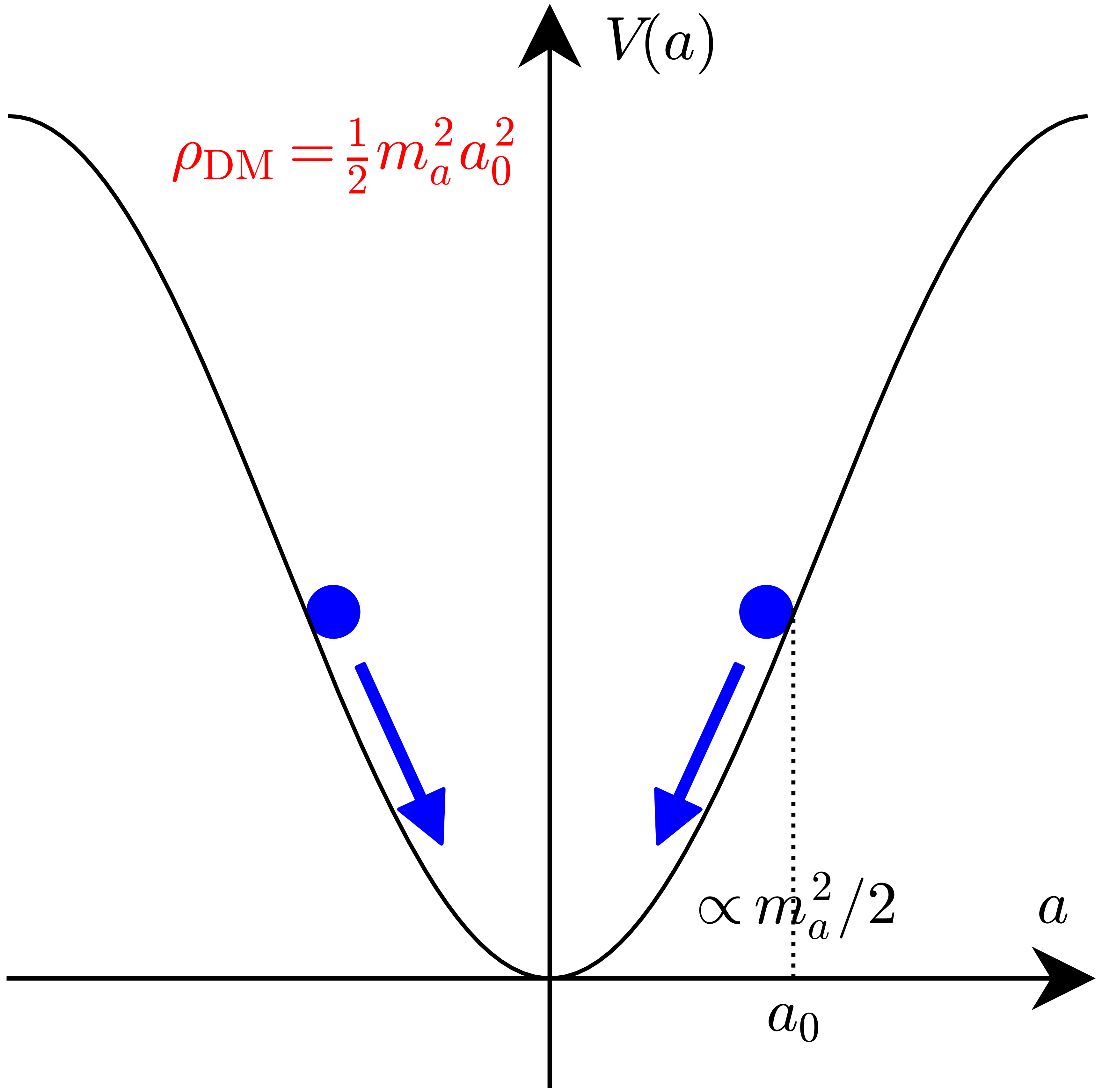

Spin dynamics for DM search

- Spin dynamics in various condensed matter systems can be used

Electron spins

- Magnons: g_{aee}

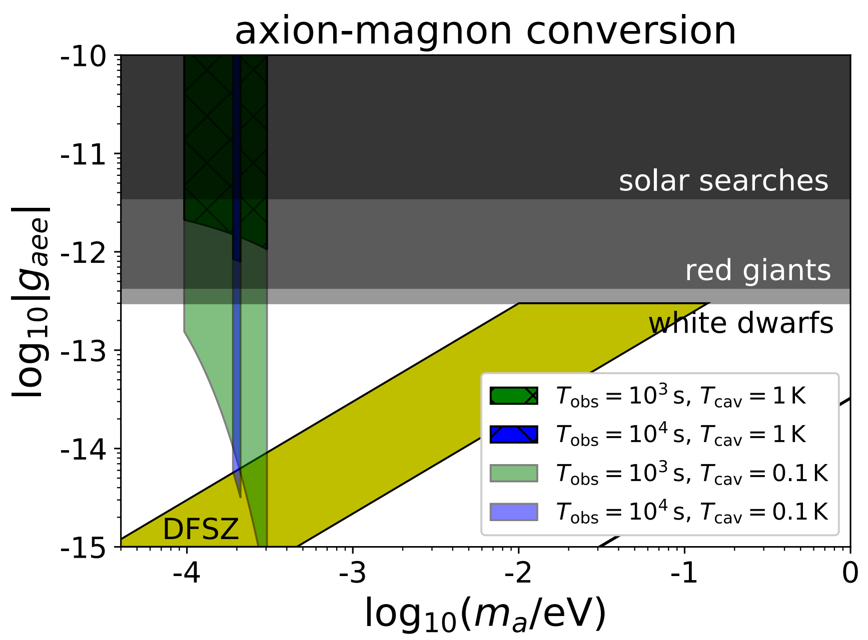

2001.10666

- Axions: $g_{a\gamma\gamma}$

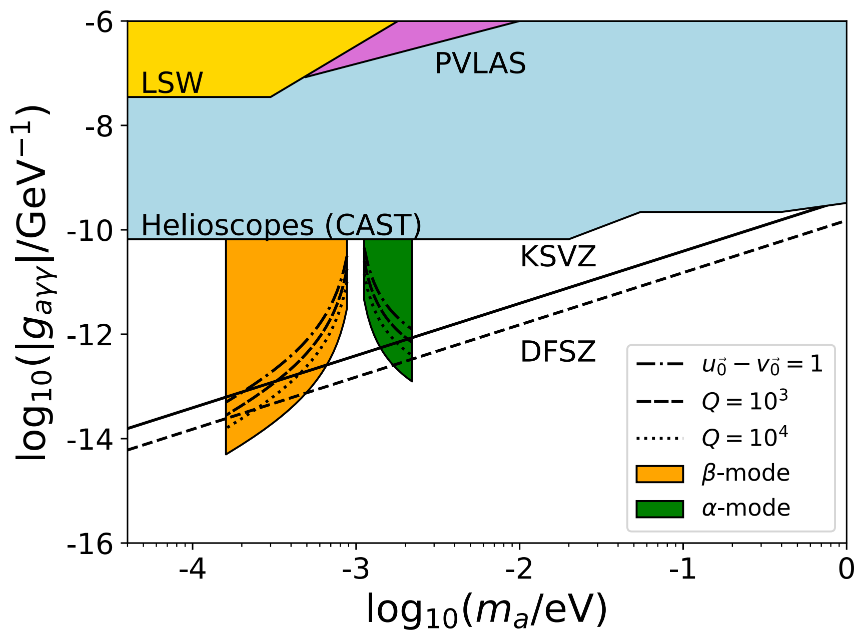

2102.06179

Nuclear spins

- superfluid $^3\mathrm{H_e}$

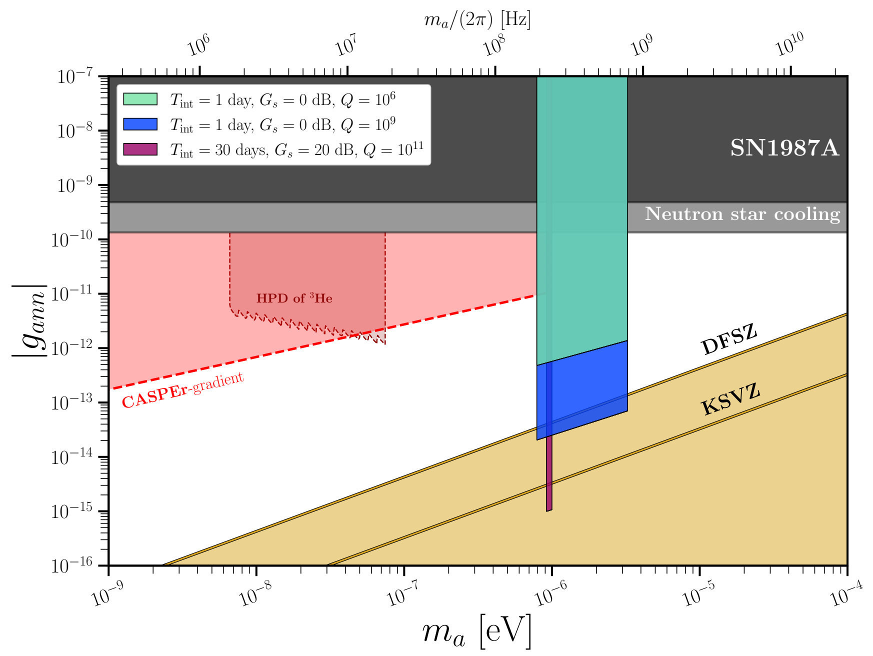

2309.09160

- hyperfine interaction

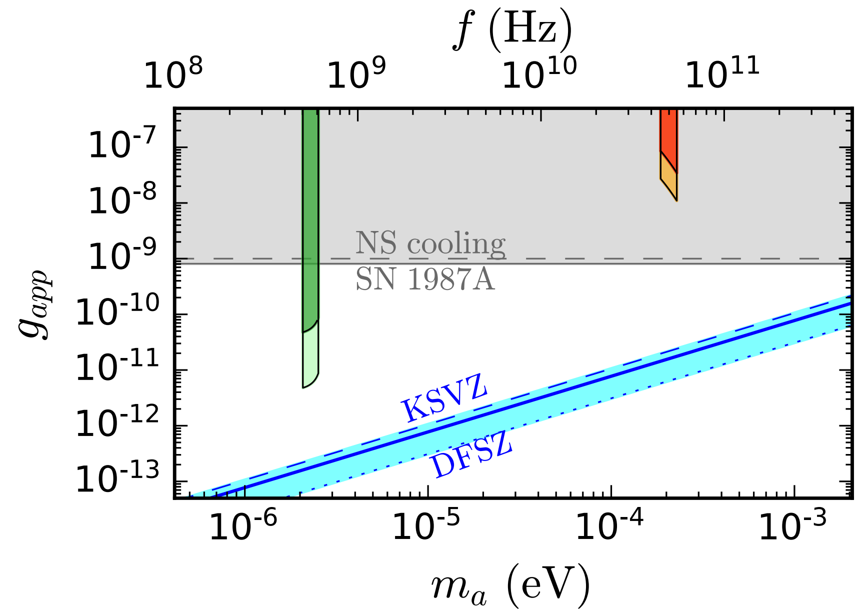

2307.08577

Today's topics

- Application of the NV center magnetometry with diamond samples 2302.12756

Brief summary of my works in this direction

Magnon as a DM signal

- Light bosonic DM converts into a collective excitation of spin = magnon

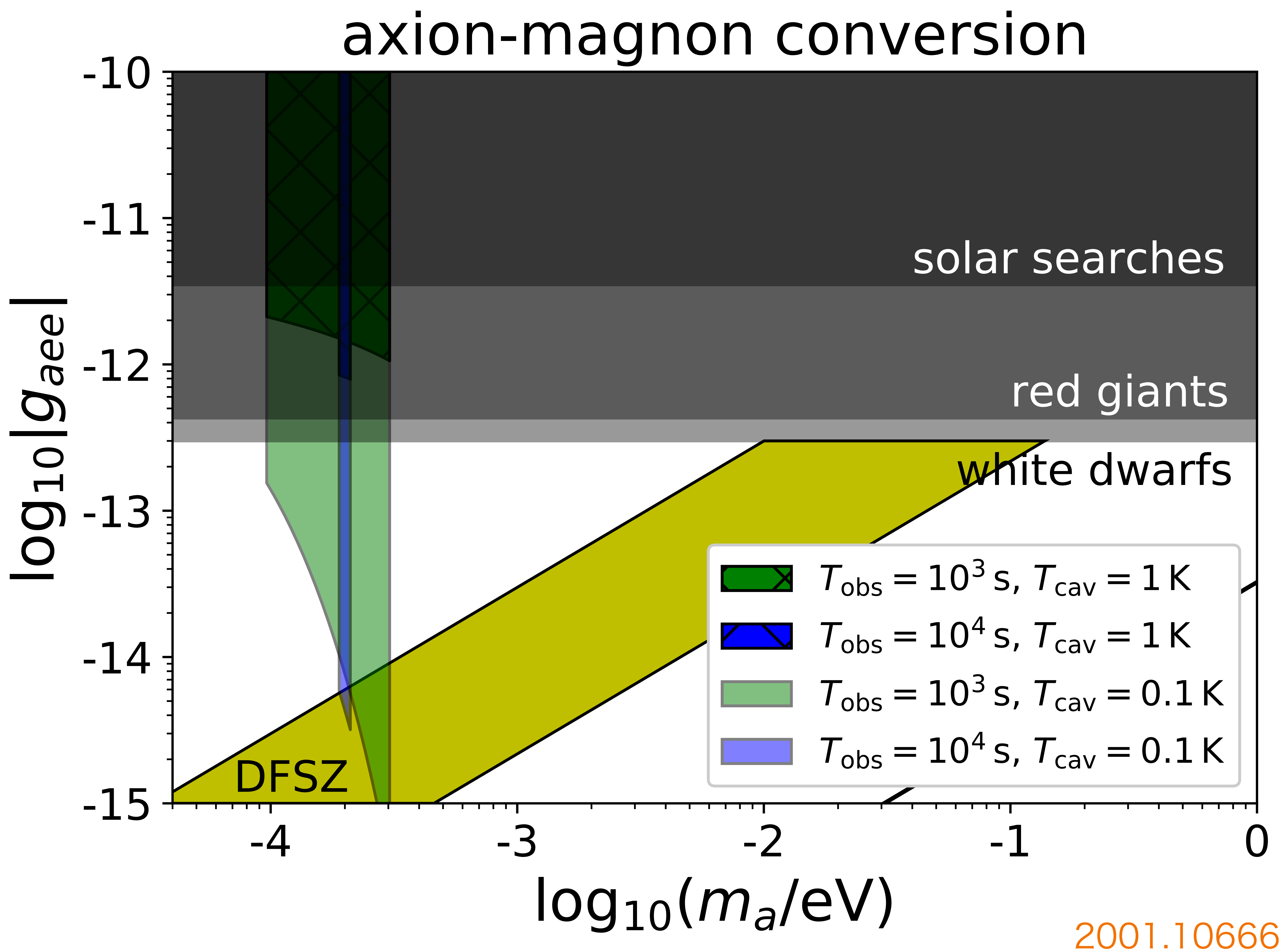

2001.10666

Table of contents

Introduction to NV center

NV center in diamond

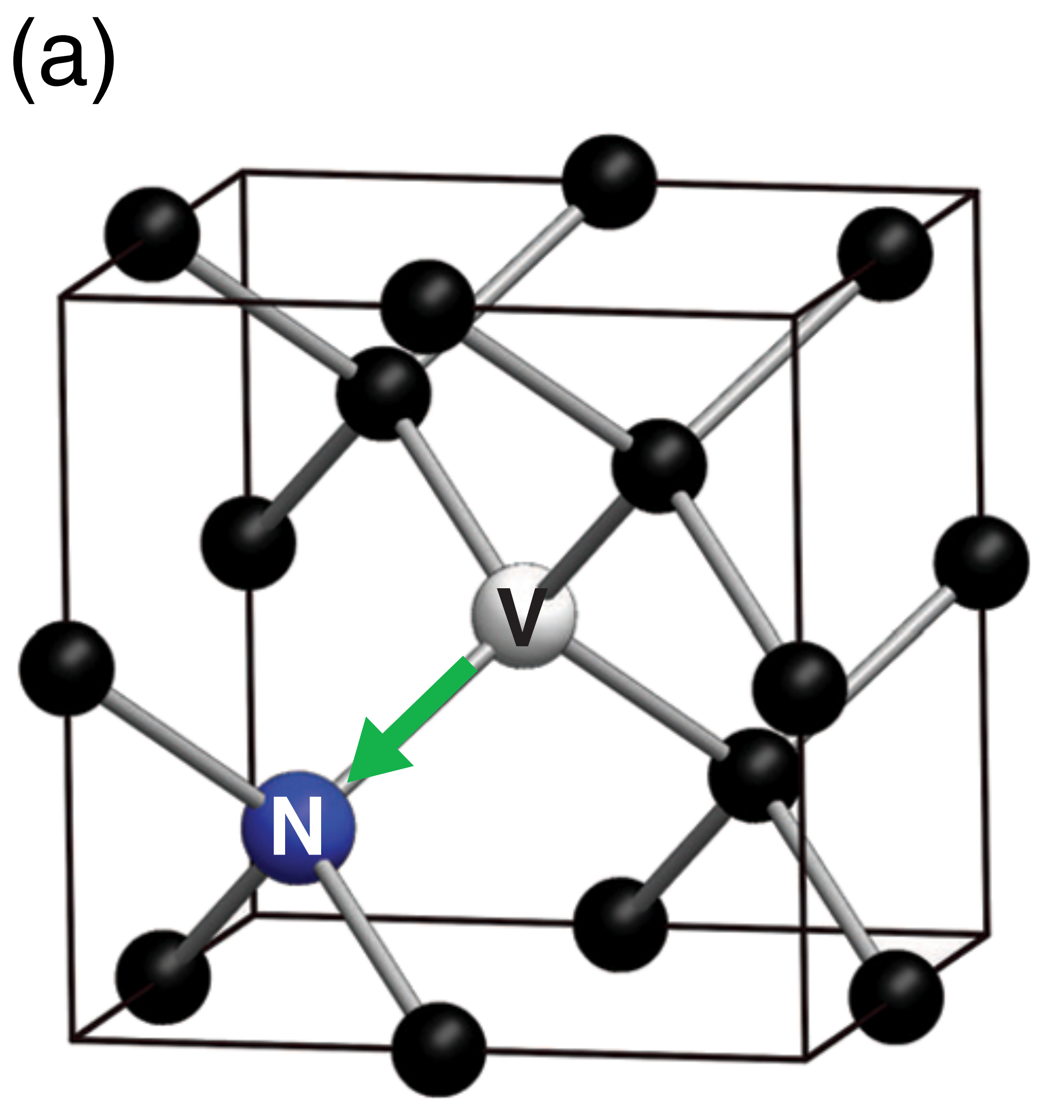

NV ∥ $[1\bar{1}\bar{1}]$ L. M. Pham '13

"pink diamond"

- The stable complex of substitutional nitrogen (N) and vacancy (V) in diamond
- The charged state NV^- has two extra e^-s localized at V
- The ground state: e^- orbital singlet, e^- spin triplet $S = 1$ system

Fluorescence

- Can distinguish spin states $|m_s = 0\rangle$ and $|m_s = \pm\rangle$ by fluorescence measurement

- Governed by following processes + selection rules
  - $^3A_2$ + 532 nm photon $\to$ ^3E
  - $^3E \to {}^3A_2$ + 600 — 850 nm photon
  - $^3E_{S\neq0} \to ({}^1A_1 \to {}^1E) \to |m_s = \pm\rangle$ + infrared photon

- The spin state $|\psi\rangle = \cos\frac{\theta}{2}|0\rangle + \sin\frac{\theta}{2}|\pm\rangle$ is read from strength of the red (pink) fluorescence light

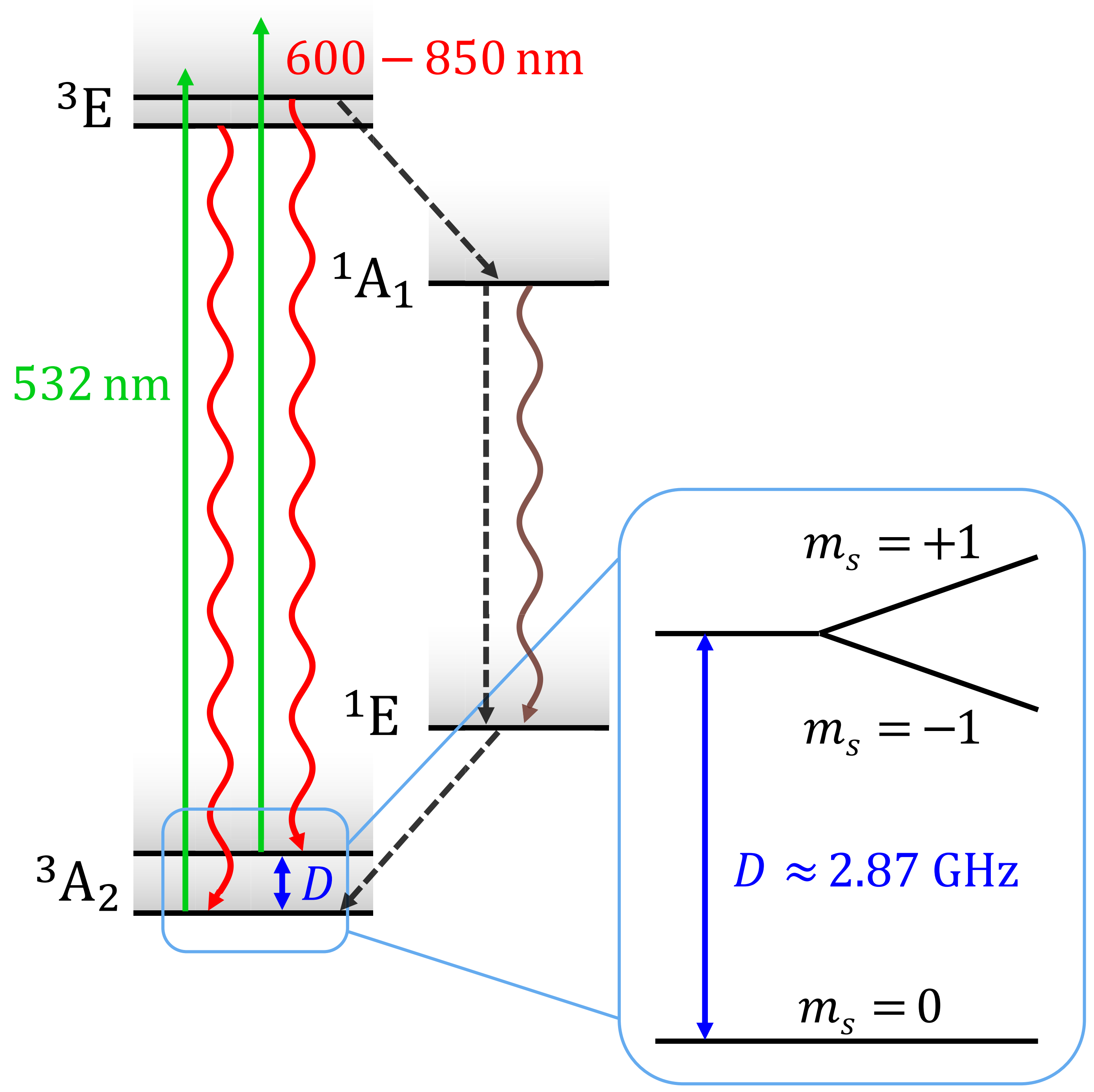

J. F. Barry+ '20

NV center as a quantum sensor

- NV center works as a multimodal quantum sensor M. W. Doherty+ [1302.3288]
  1. Temperature G. Kucsko+ '13
  2. Electric field F. Dolde+ '11
  3. Strain M. Barson+ '17
  4. Magnetic field (explain later)
     - No cryogenics
     - No vacuum system
     - No tesla-scale applied bias fields are required

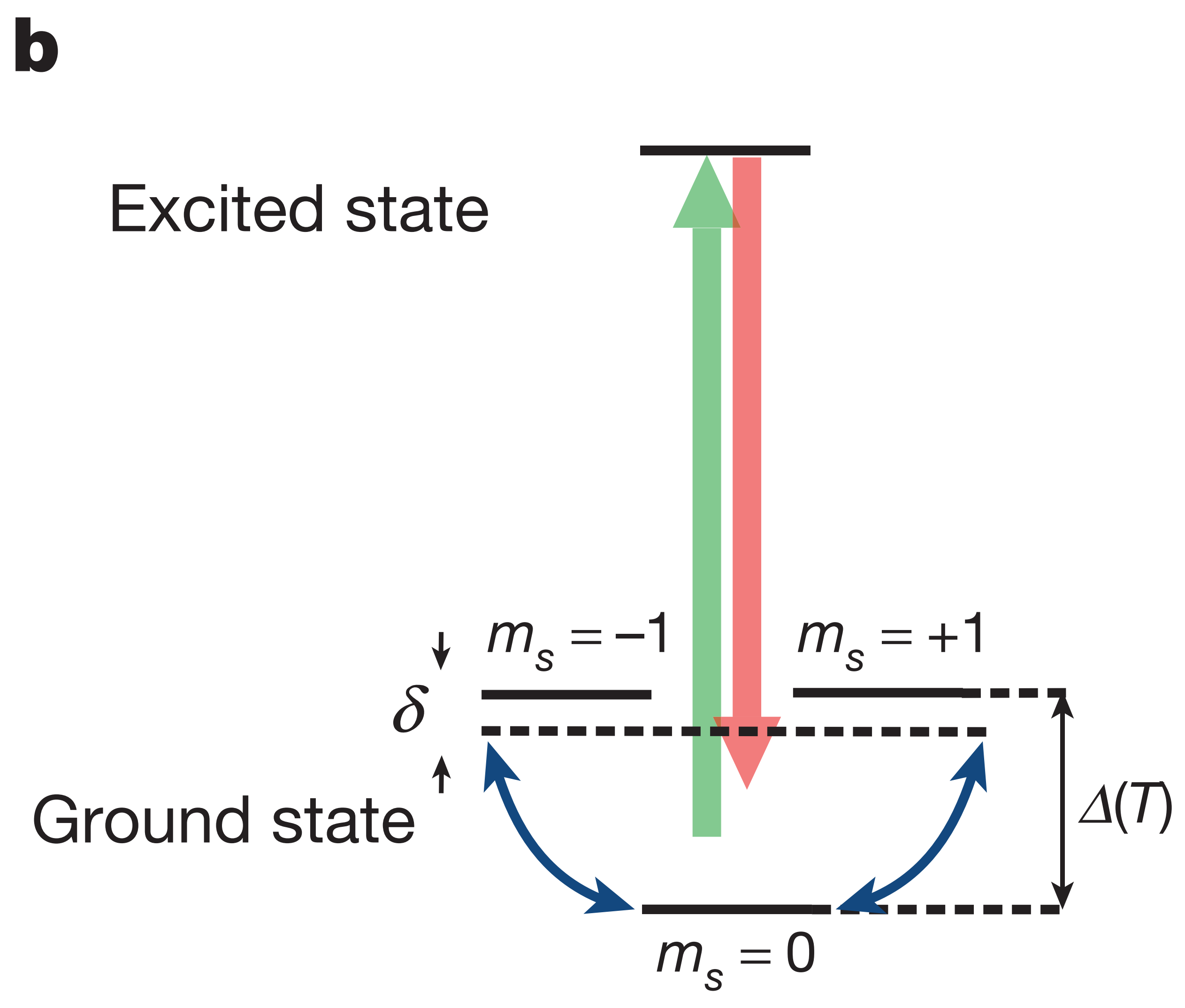

- Two options
  - Single NV center (high spacial resolution)
  - Ensemble of NV centers (high sensitivity) with $\sim 1 - 20\,\mathrm{ppm}$ concentration

Applications of NV center magnetometory

- Single NV center
  - $B_{ac} \sim 9.1\,\mathrm{nT\,Hz^{-1/2}}$
  - $B_{dc} \sim 10\,\mathrm{nT\,Hz^{-1/2}}$

  D. Herbschleb+ '19

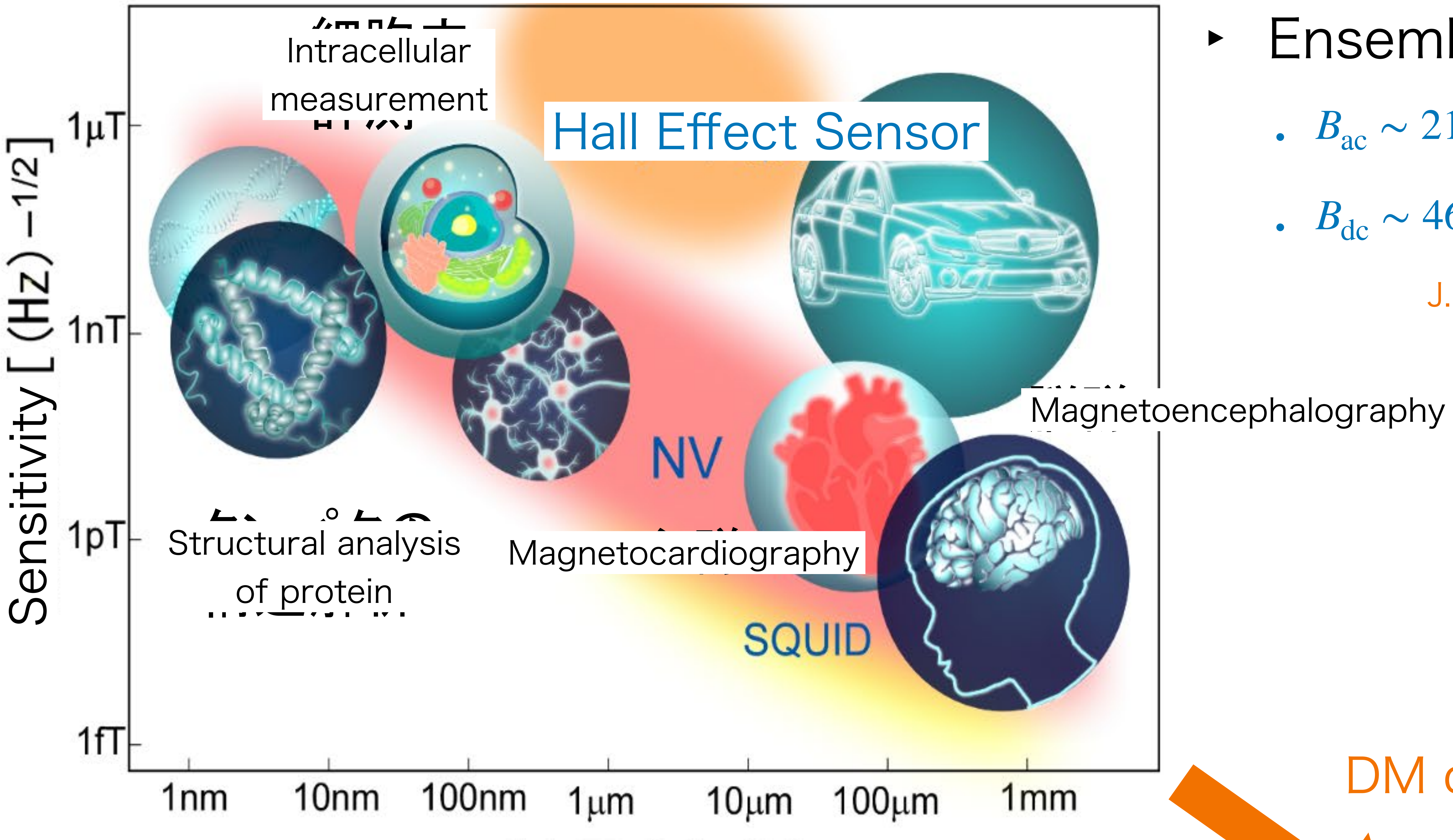

水落, 応用物理, 87, 251-261(2018).

- Ensemble
  - $B_{ac} \sim 210\,\mathrm{fT\,Hz^{-1/2}}$
  - $B_{dc} \sim 460\,\mathrm{fT\,Hz^{-1/2}}$

  J. F. Barry+ '23

DM detection :)

DC magnetometry

Rabi cycle

- Energy gap $\Delta E \sim 2\pi \times 2.87\,\mathrm{GHz}$
- Inject oscillating driving field with frequency $f = D + \frac{1}{2\pi}\gamma_e B_z$
  - $|-\rangle$ is irrelevant
  - qubit system of $|0\rangle$ and $|+\rangle$

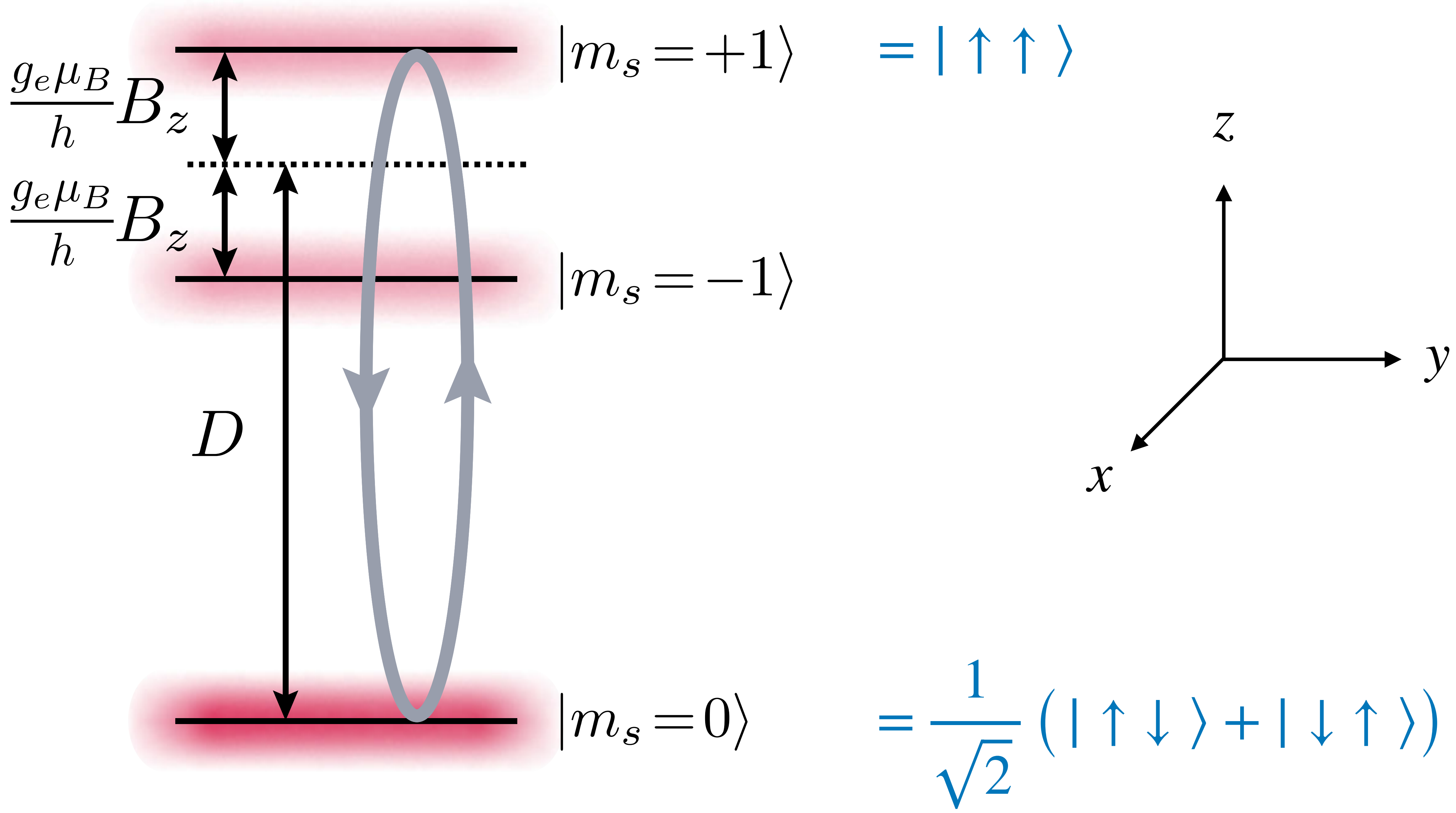

J. F. Barry+ '20

- Under the transverse magnetic field $\mathbf{B}_1 = B_{1y}\,\hat{\mathbf{y}}\sin(2\pi f t)$,

Time evolution is described by the Rabi cycle

$$|\psi(t)\rangle = \cos\left(\frac{1}{\sqrt{2}}\gamma_e B_{1y}\,t\right)|0\rangle + \sin\left(\frac{1}{\sqrt{2}}\gamma_e B_{1y}\,t\right)|+\rangle$$

Bloch sphere

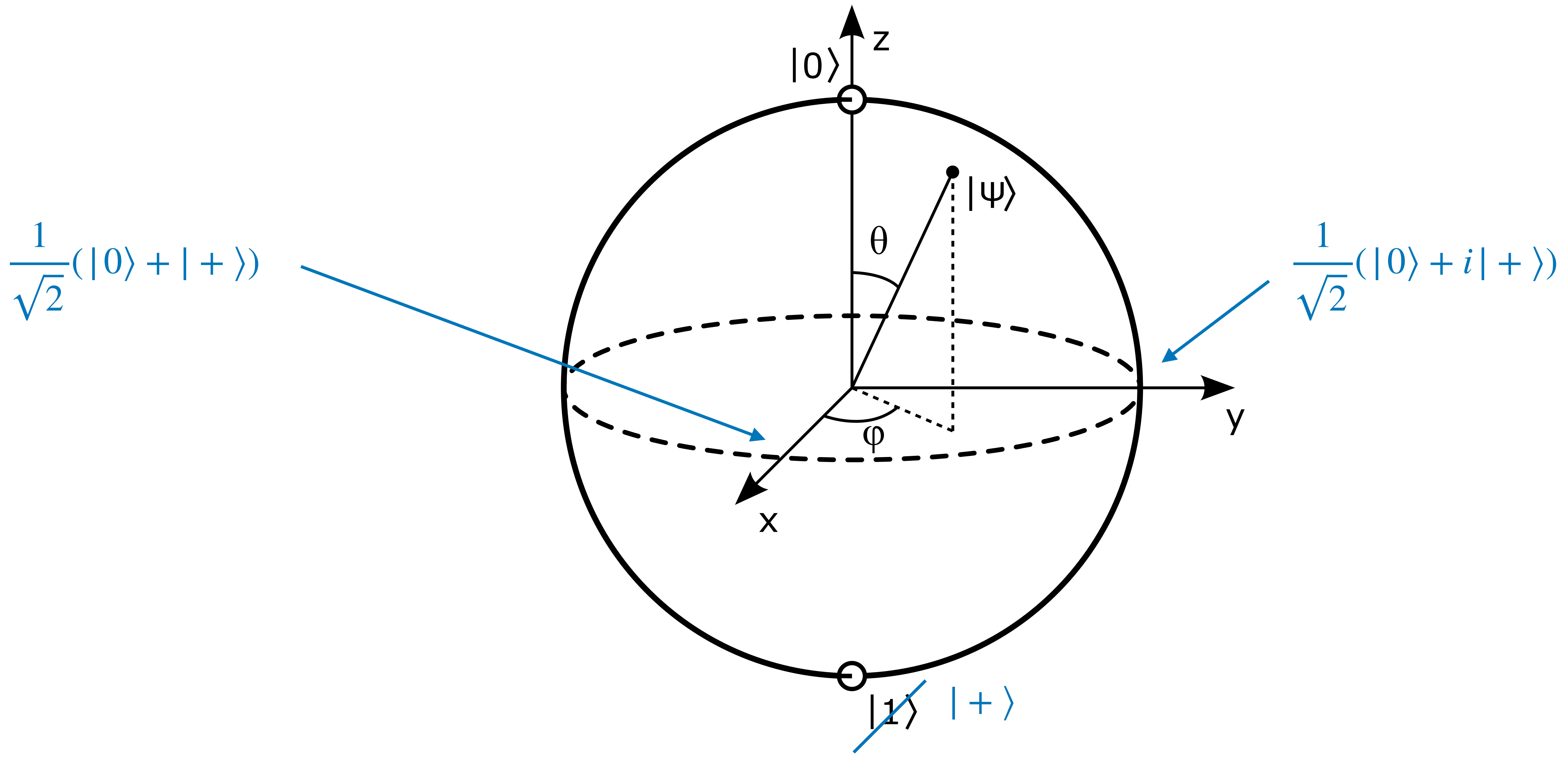

- Map from SU(2) group elements to the sphere S^2

$$|\psi\rangle = \cos\frac{\theta}{2}|0\rangle + \sin\frac{\theta}{2}e^{i\varphi}|+\rangle = \left(|0\rangle \quad |+\rangle\right)\begin{pmatrix} \cos\frac{\theta}{2} & -\sin\frac{\theta}{2}e^{-i\varphi} \\ \sin\frac{\theta}{2}e^{i\varphi} & \cos\frac{\theta}{2} \end{pmatrix}\begin{pmatrix} 1 \\ 0 \end{pmatrix}$$

Rabi cycle on Bloch sphere

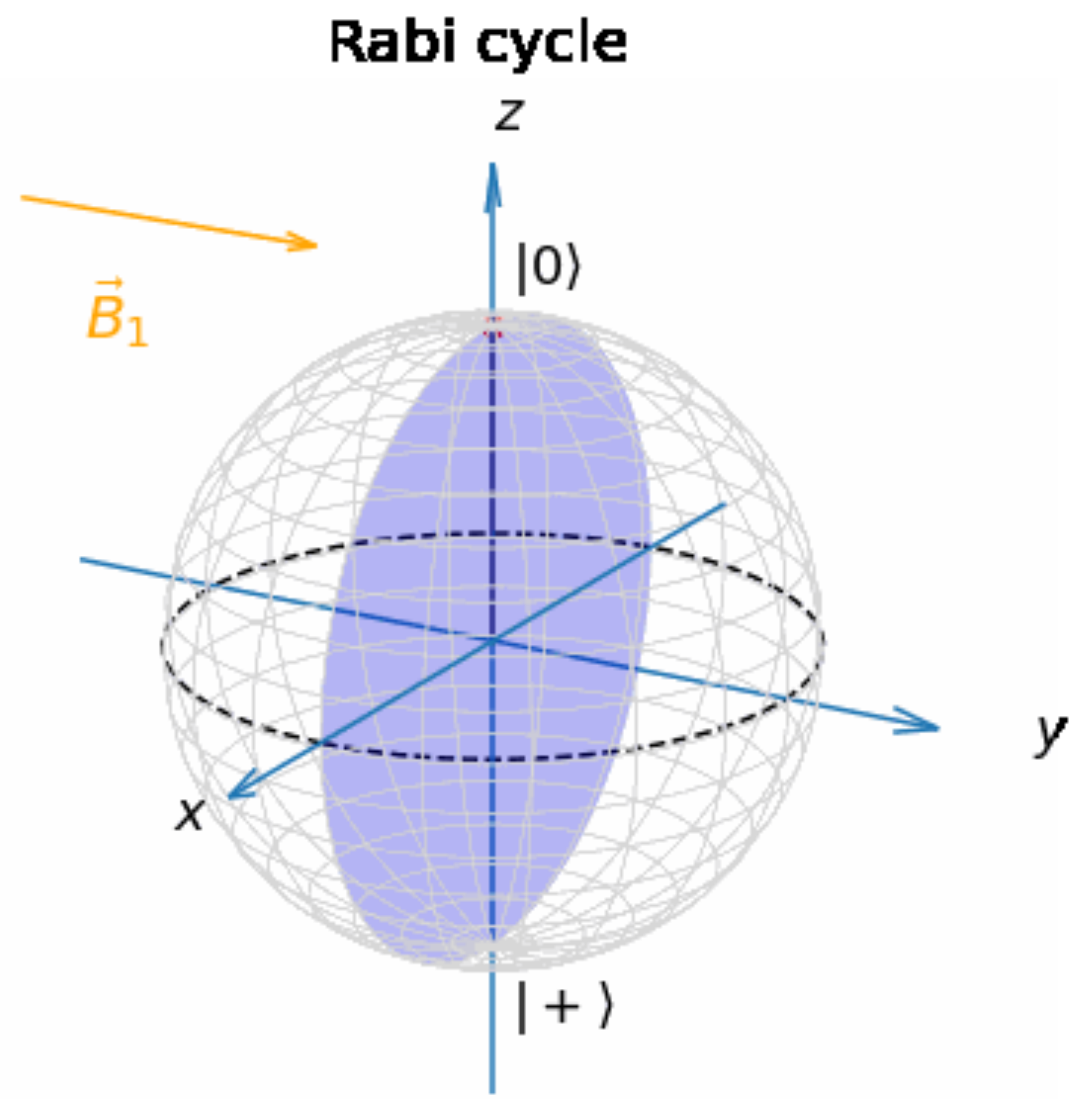

- Rotation around $\vec{B}_1 \propto \hat{\mathbf{y}}$

$$|\psi(t)\rangle = \cos\frac{\theta(t)}{2}|0\rangle + \sin\frac{\theta(t)}{2}|+\rangle \text{ with } \theta(t) = \sqrt{2}\gamma_e B_{1y}\, t$$

Free precession

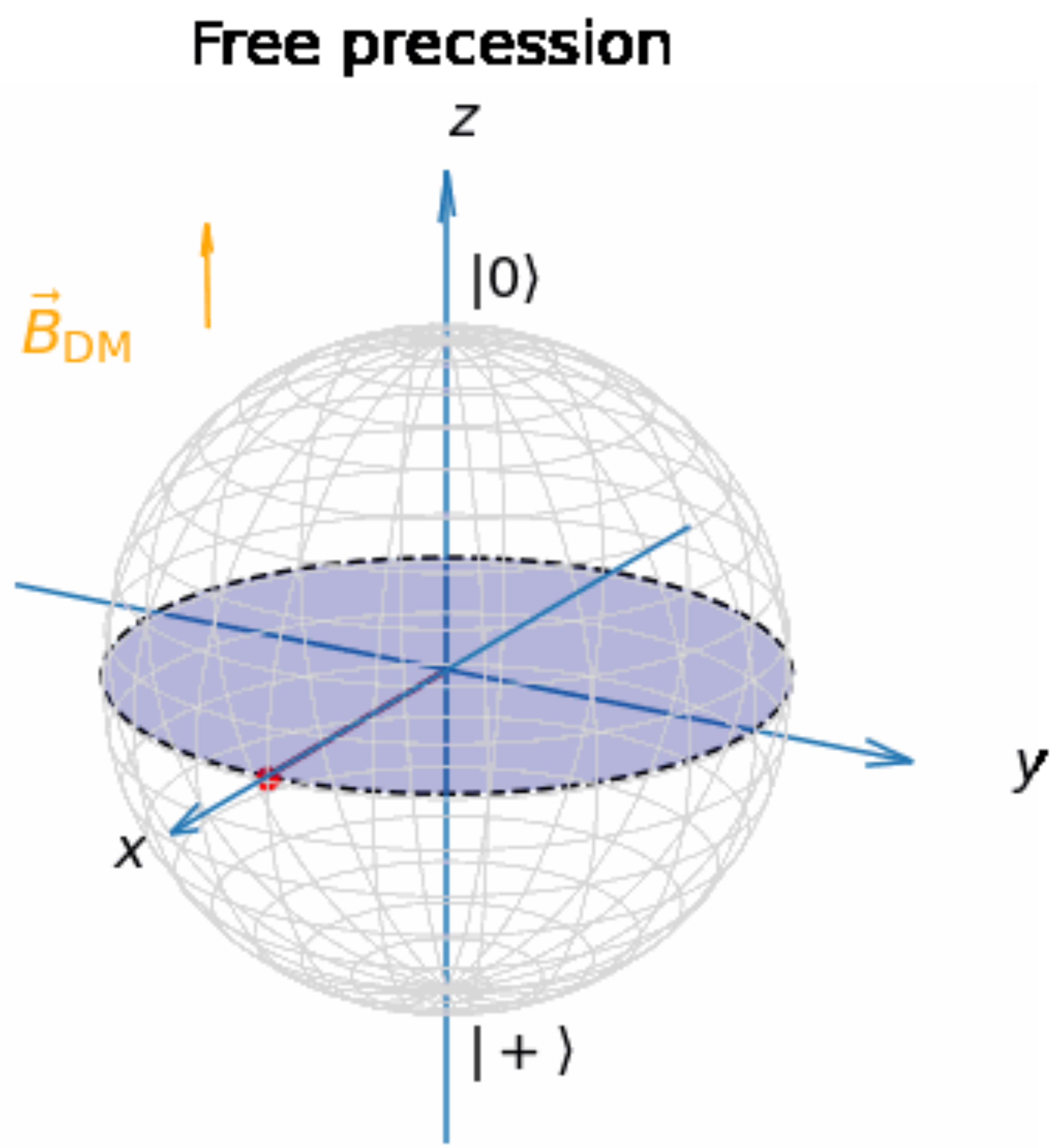

- Magnetic field $\vec{B} \propto \hat{z}$ causes free precession = rotation around $\hat{\mathbf{z}}$

$|\psi(\tau)\rangle = \frac{1}{\sqrt{2}}\left(|0\rangle + e^{i\varphi(\tau)}|+\rangle\right)$ with $\varphi(\tau) = \gamma_e \int_0^\tau dt\, B^z_{\rm DM}(t) \simeq \gamma_e B^z_{\rm DM}\tau$ (for DC-like signal)

Ramsey sequence

Ramsey sequence for DC magnetometry

1. $(\pi/2)_y$ pulse
    - Rabi cycle with $\theta = \sqrt{2}\gamma_e B_{1y} t = \pi/2$
2. Free precession under $\mathbf{B}_{\rm DM}$ for duration $\tau \sim T_2^*/2$
    - $T_2^* \sim 1\,\mu{\rm s}$: spin relaxation (dephasing) time
3. $(\pi/2)_x$ pulse
4. Fluorescence measurement
    - DM signal is population difference between $|0\rangle$ and $|+\rangle$

$$S \equiv \frac{1}{2}\langle \psi_{\rm fin.} | \sigma_z | \psi_{\rm fin.} \rangle \propto \varphi(\tau) = \gamma_e B^z_{\rm DM} \tau \quad (\varphi(\tau) \ll 1)$$

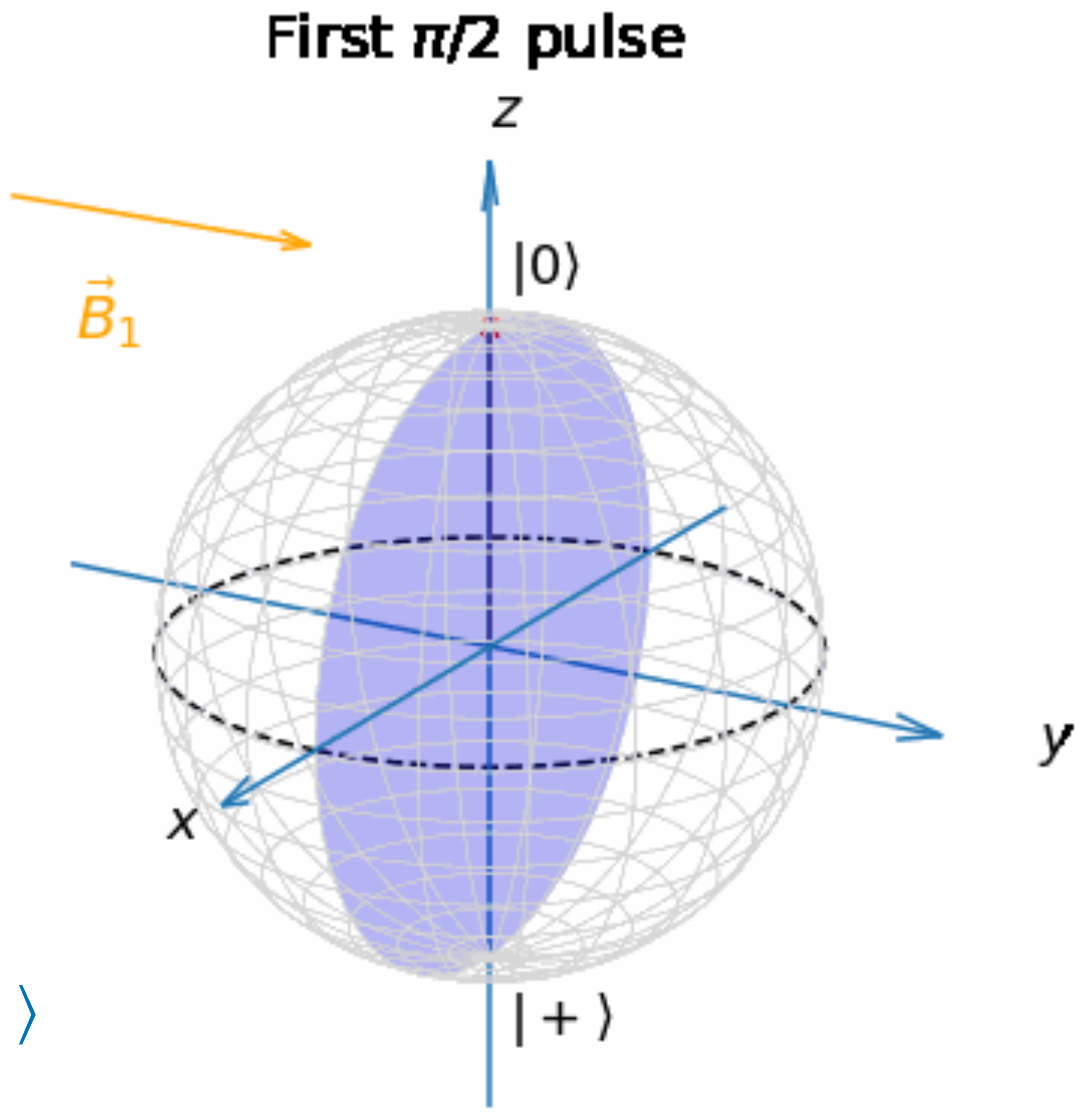

Sensitivity on axion DM

- Assume spin-projection noise limits the sensitivity

$$|x\rangle \equiv \frac{1}{\sqrt{2}}\left(|0\rangle + |+\rangle\right)$$

$$\Delta S \equiv \frac{1}{2}\left[\langle x|\sigma_z^2|x\rangle - \left(\langle x|\sigma_z|x\rangle\right)^2\right]^{1/2} = \frac{1}{2}$$

- Large statistics reduce noise
  - N : # of NV centers
  - $t_{\rm obs}$: total observation time

- (Roughly) universally sensitive to dc-like signal with $m \lesssim 2\pi/\tau \sim 10^{-8}\,{\rm eV}$

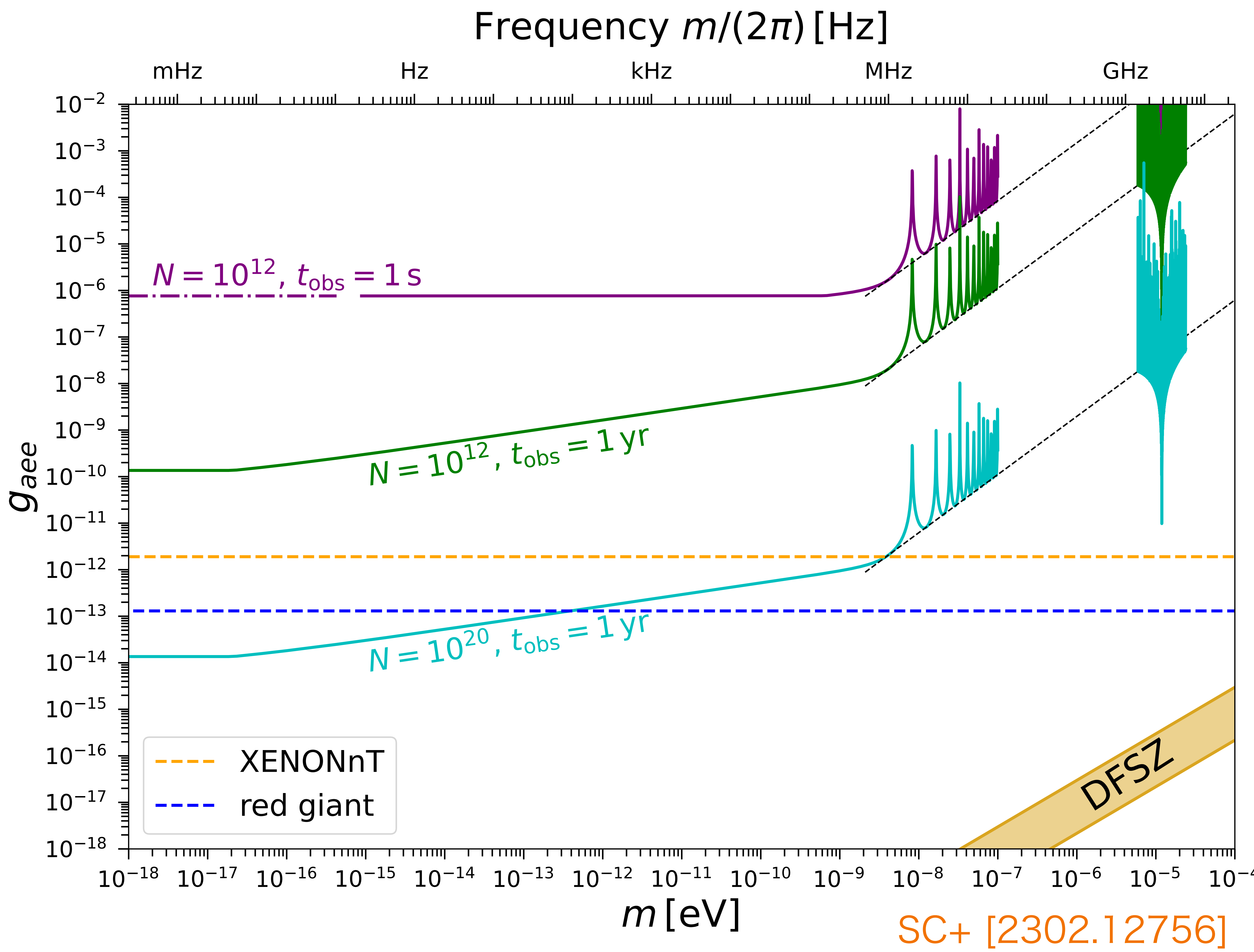

SC+ [2302.12756]

Effects of DM coherence time

- $B^z_{\rm DM}$ and δ change randomly with $\tau_{\rm DM} \sim 2\pi/m_{\rm DM} v^2_{\rm DM}$
- For $t_{\rm obs} \ll \tau_{\rm DM}$
  - Fixed $B^z_{\rm DM}$ and δ
  - (# of observations) $\simeq N\left(t_{\rm obs}/\tau\right)$
  - (Sensitivity) $\propto N^{1/2}\left(t_{\rm obs}/\tau\right)^{1/2}$
- For $t_{\rm obs} \gg \tau_{\rm DM}$
  - We measure the variance of $S_{\rm obs}$
  - Comparison of $\Delta S_{\rm DM}$ and $\Delta S\, N^{-1/2}\left(\tau_{\rm DM}/\tau\right)^{-1/2}$
  - (Sensitivity) $\propto N^{1/2}\left(\tau_{\rm DM}/\tau\right)^{1/2}\left(t_{\rm obs}/\tau_{\rm DM}\right)^{1/4}$

    Consistent with Dror+ [2210.06481] in the context of CASPEr

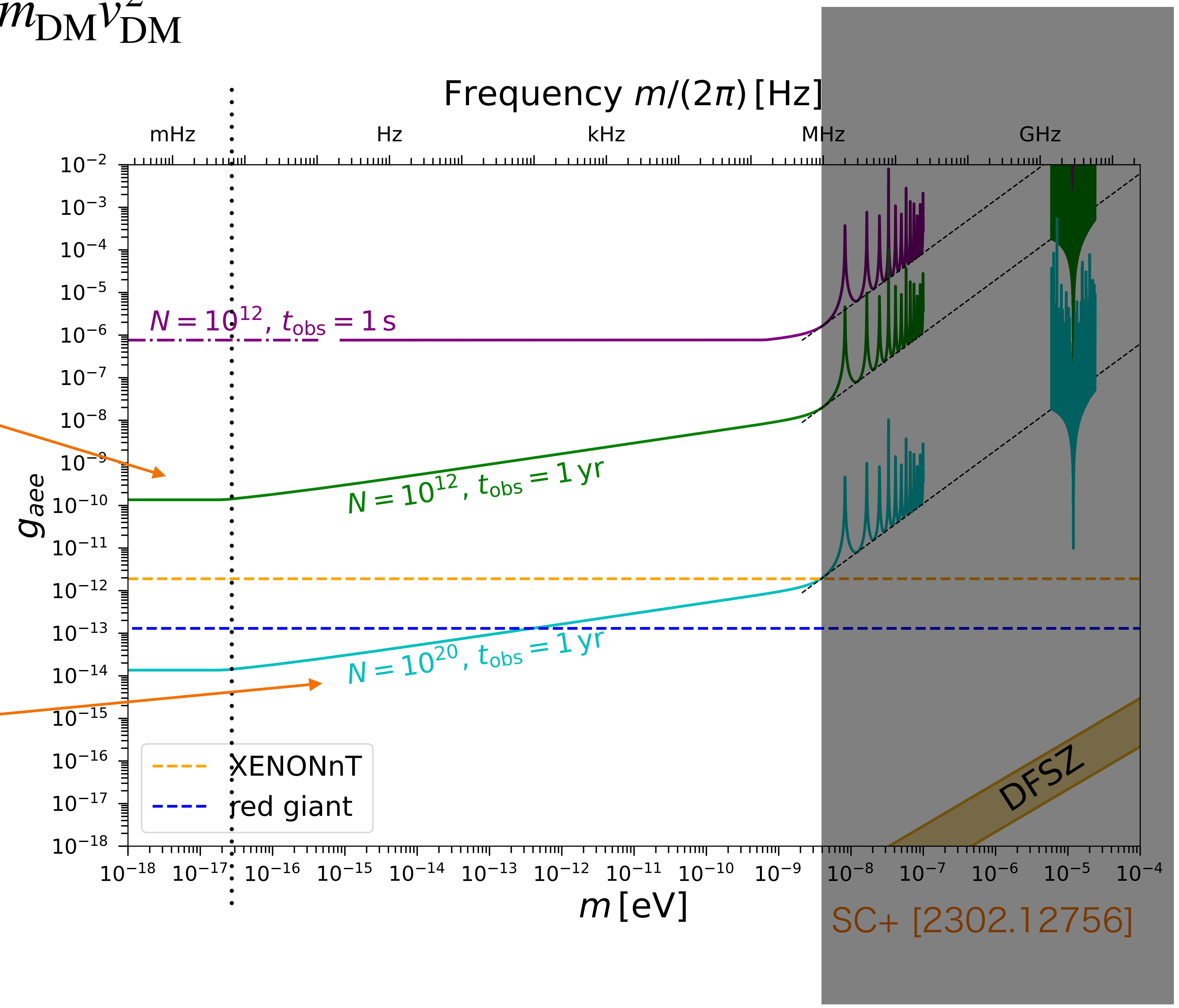

Insensitive to fast-oscillating signals

- Fast oscillation leads to cancellation

$$S \sim \int_0^\tau dt\, B^z_{\rm DM} \sin(mt) \propto \frac{1-\cos(m\tau)}{m\tau}$$

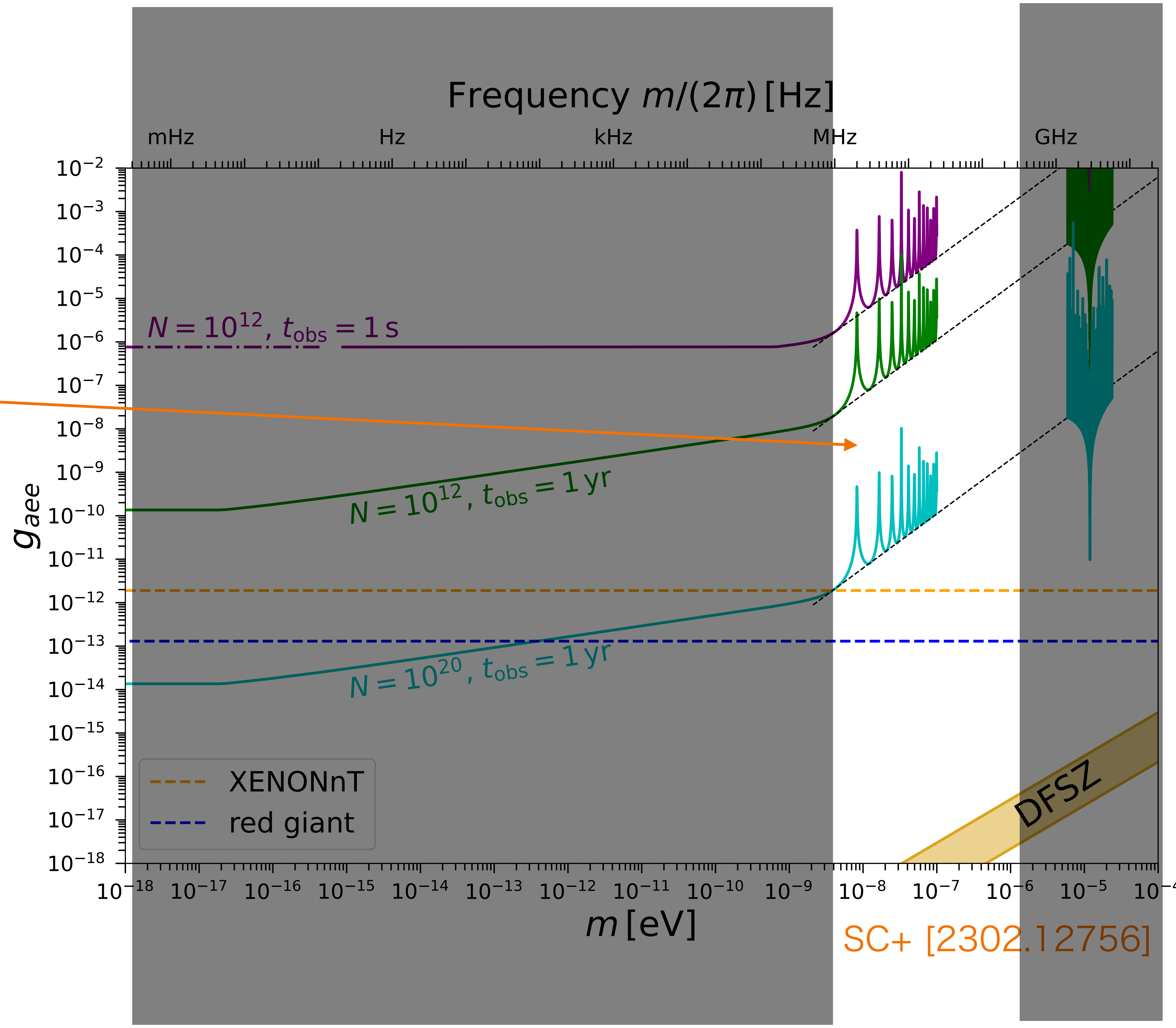

SC+ [2302.12756]

DM on resonance

If $m/2\pi \simeq f$, DM field itself works as a driving field

"Resonance" sequence for $m/2\pi \simeq f$

1. $(\pi/2)_y$ pulse
2. Free precession for duration $\tau \sim T_2^*/2$
3. Fluorescence measurement

   $S \propto B_{\rm DM}^y \tau$

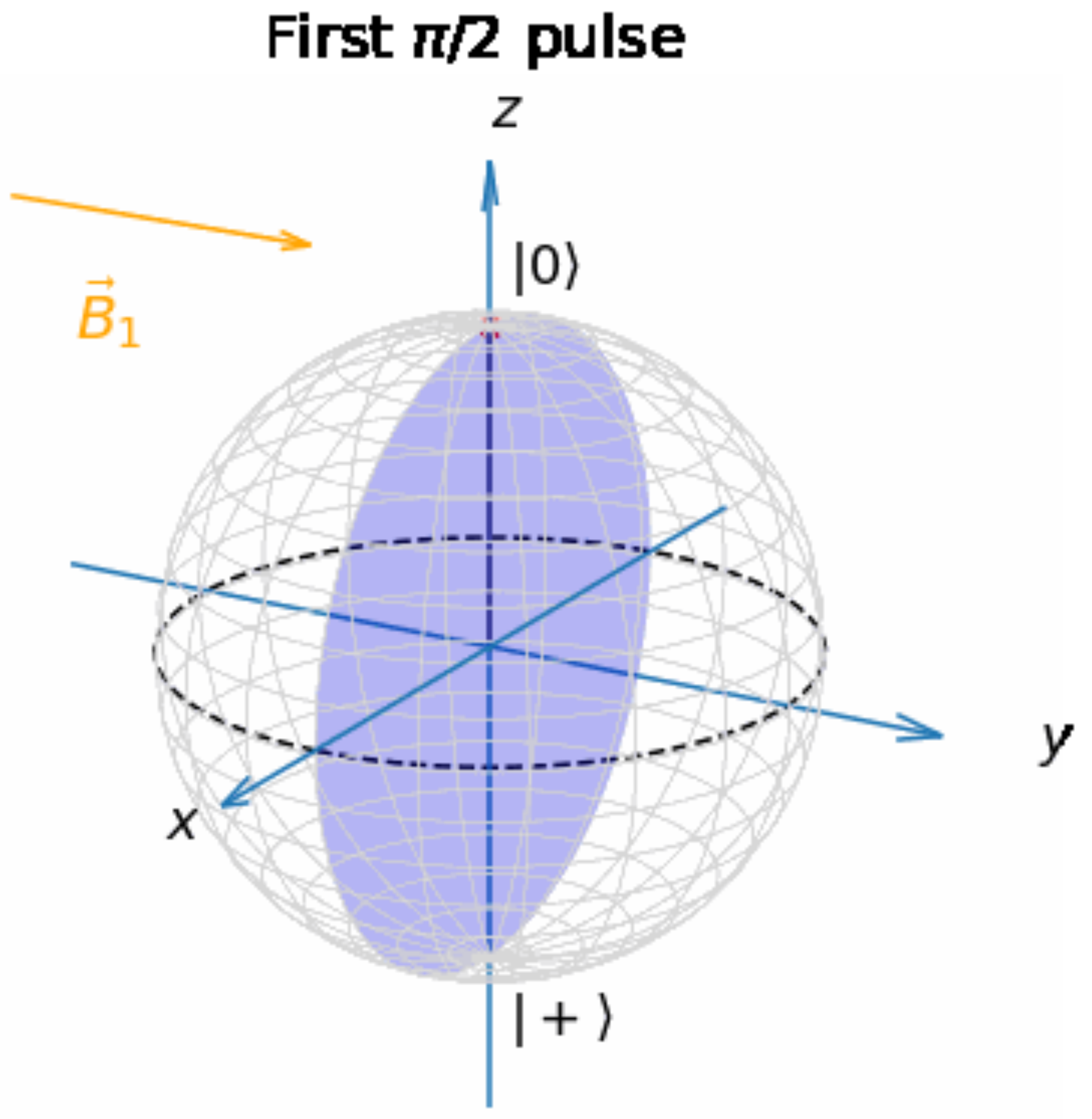

On resonance sensitivity

- Resonance position

  $$\frac{m}{2\pi} \simeq 2.87\,\mathrm{GHz} \Leftrightarrow m \simeq 11.9\,\mu\mathrm{eV}$$

  - Tunable with e.g., external magnetic field $\mathbf{B}$

- Resonant enhancement of sensitivity w/

  $$m\tau \sim 2 \times 10^4 \left(\frac{\tau}{1\,\mu\mathrm{s}} \right)$$

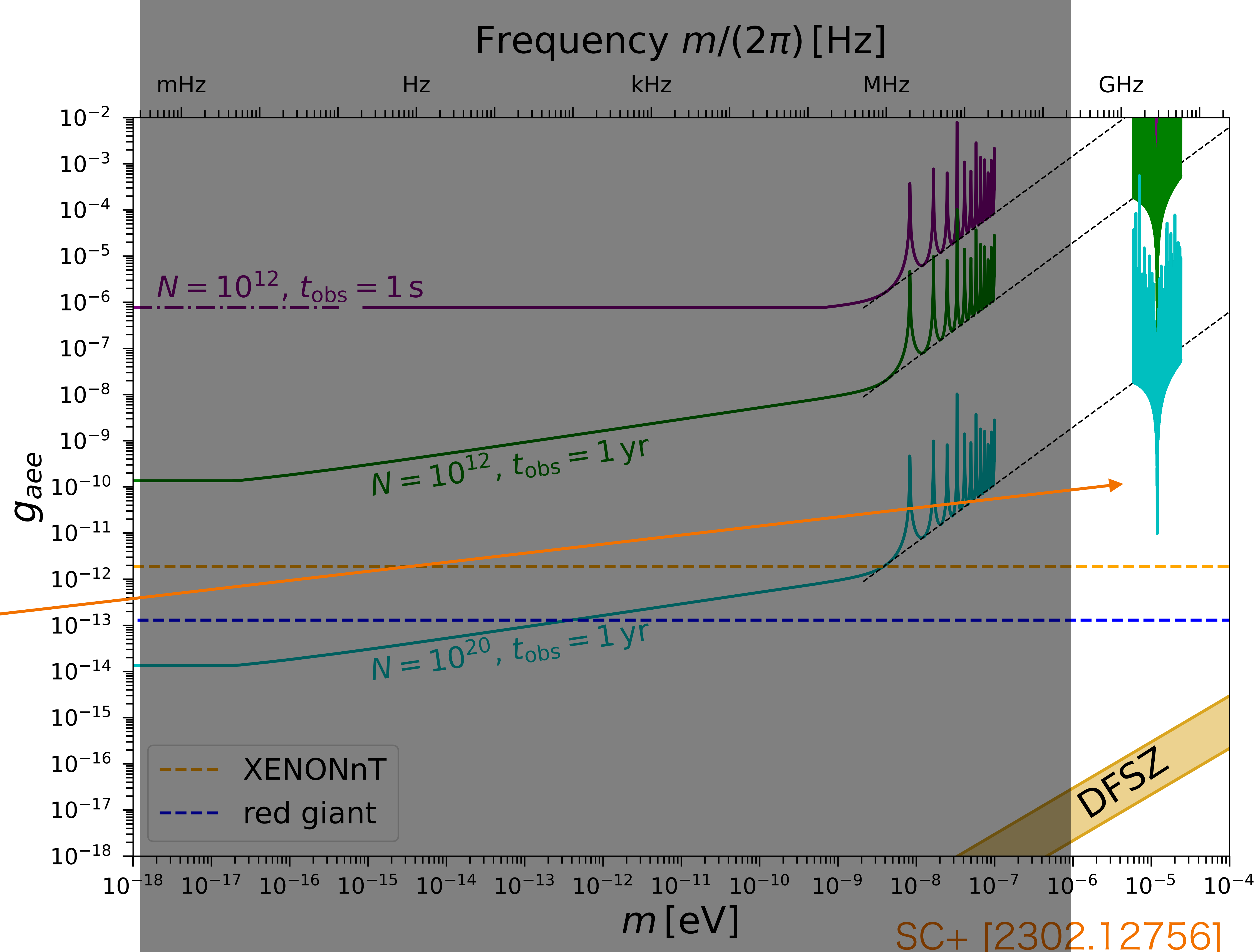

SC+ [2302.12756]

AC magnetometry

Insensitive to fast-oscillating signals

- Fast oscillation leads to cancellation when $m \lesssim 2\pi/\tau$

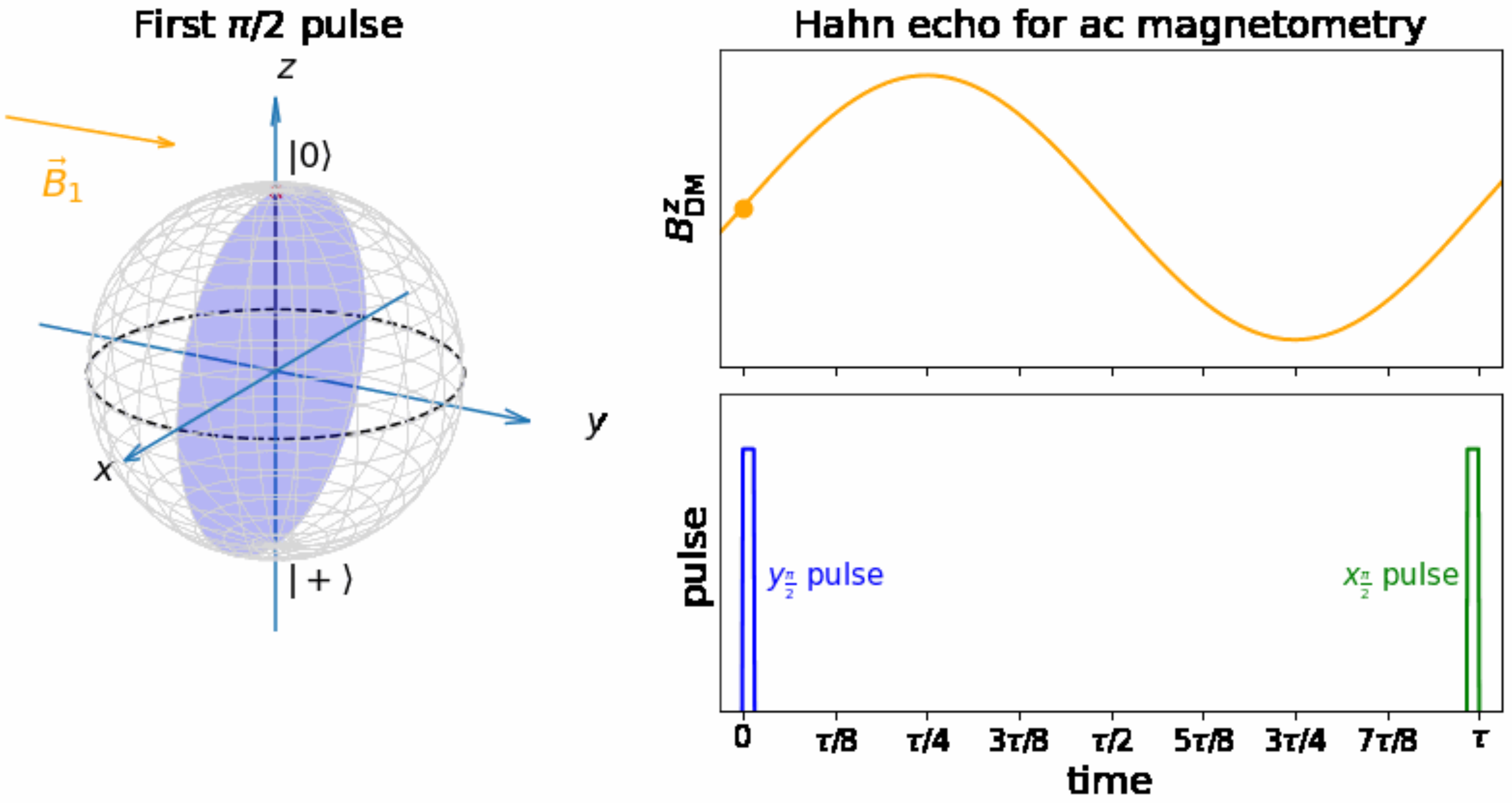

Hahn echo

Hahn echo for ac magnetometry

1. $(\pi/2)_y$ pulse
2. Free precession for $\tau/2$
3. π_y pulse
4. Free precession for $\tau/2$
5. $(\pi/2)_x$ pulse
6. Fluorescence measurement

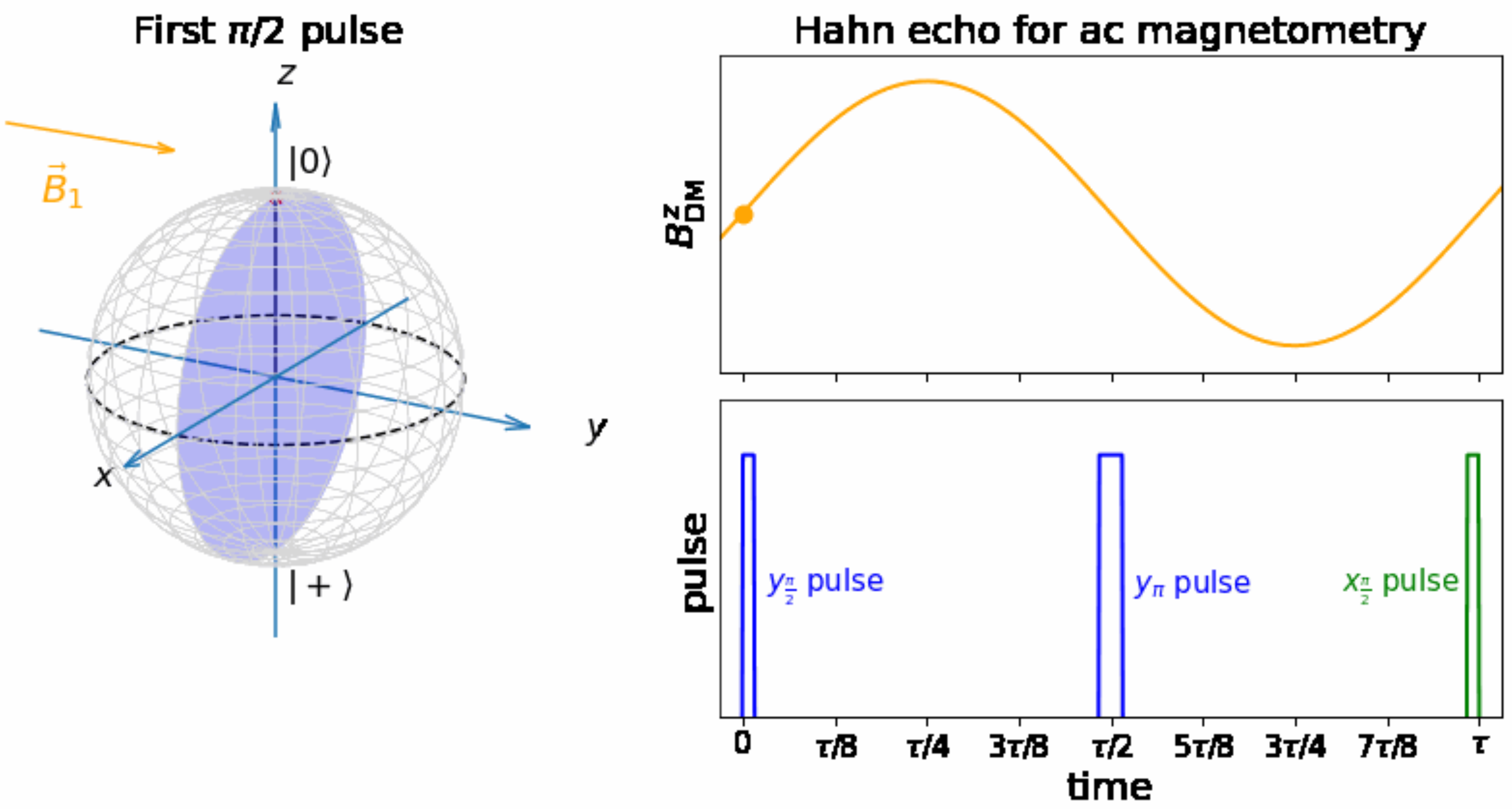

$$\varphi(\tau) = \gamma_e\left(\int_0^{\tau/2} dt\, B^z_{\rm DM}(t) - \int_{\tau/2}^{\tau} dt\, B^z_{\rm DM}(t)\right) \Longrightarrow$$ Targeted at the frequency $\sim 1/\tau$

Prolonged relaxation time

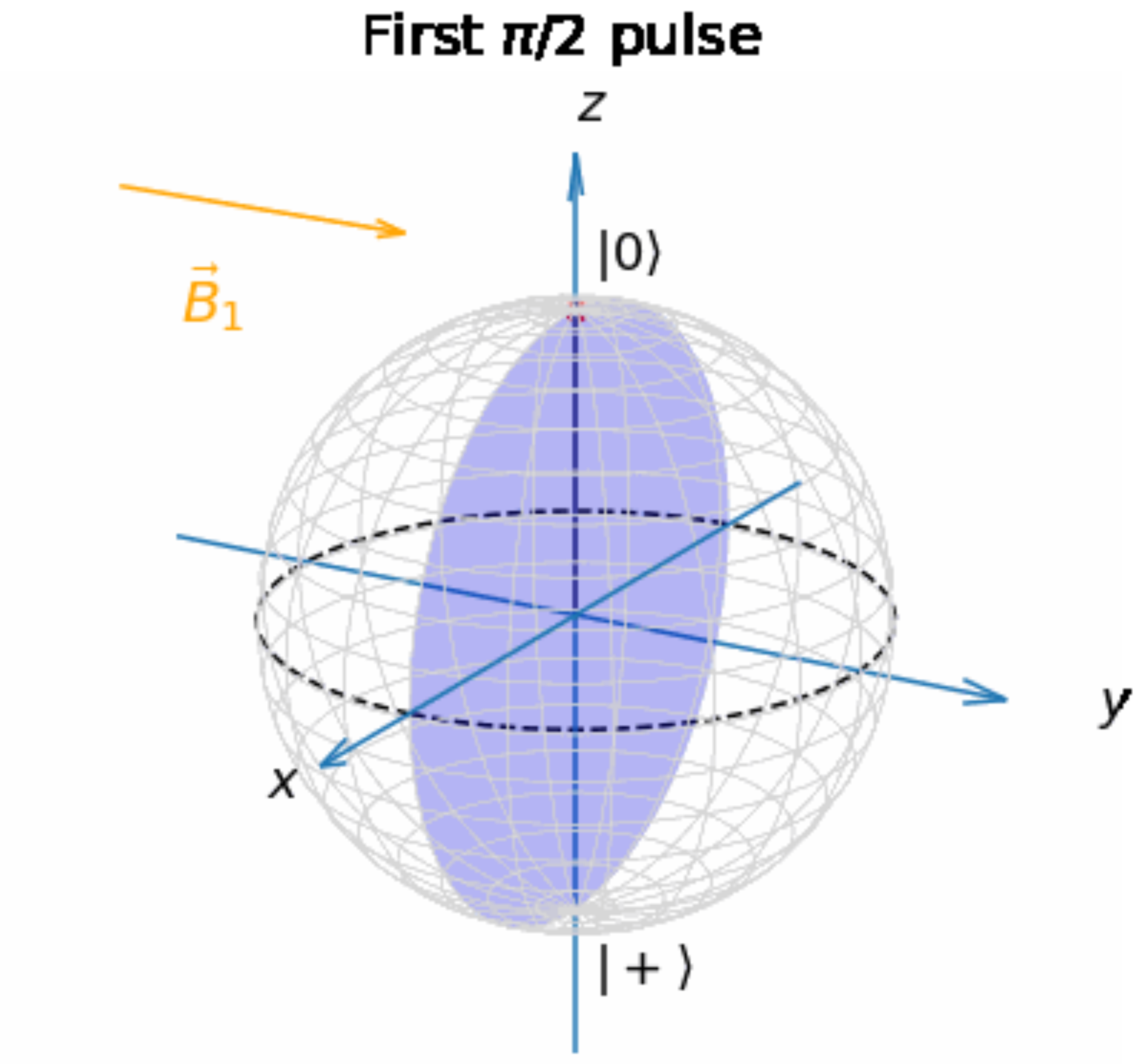

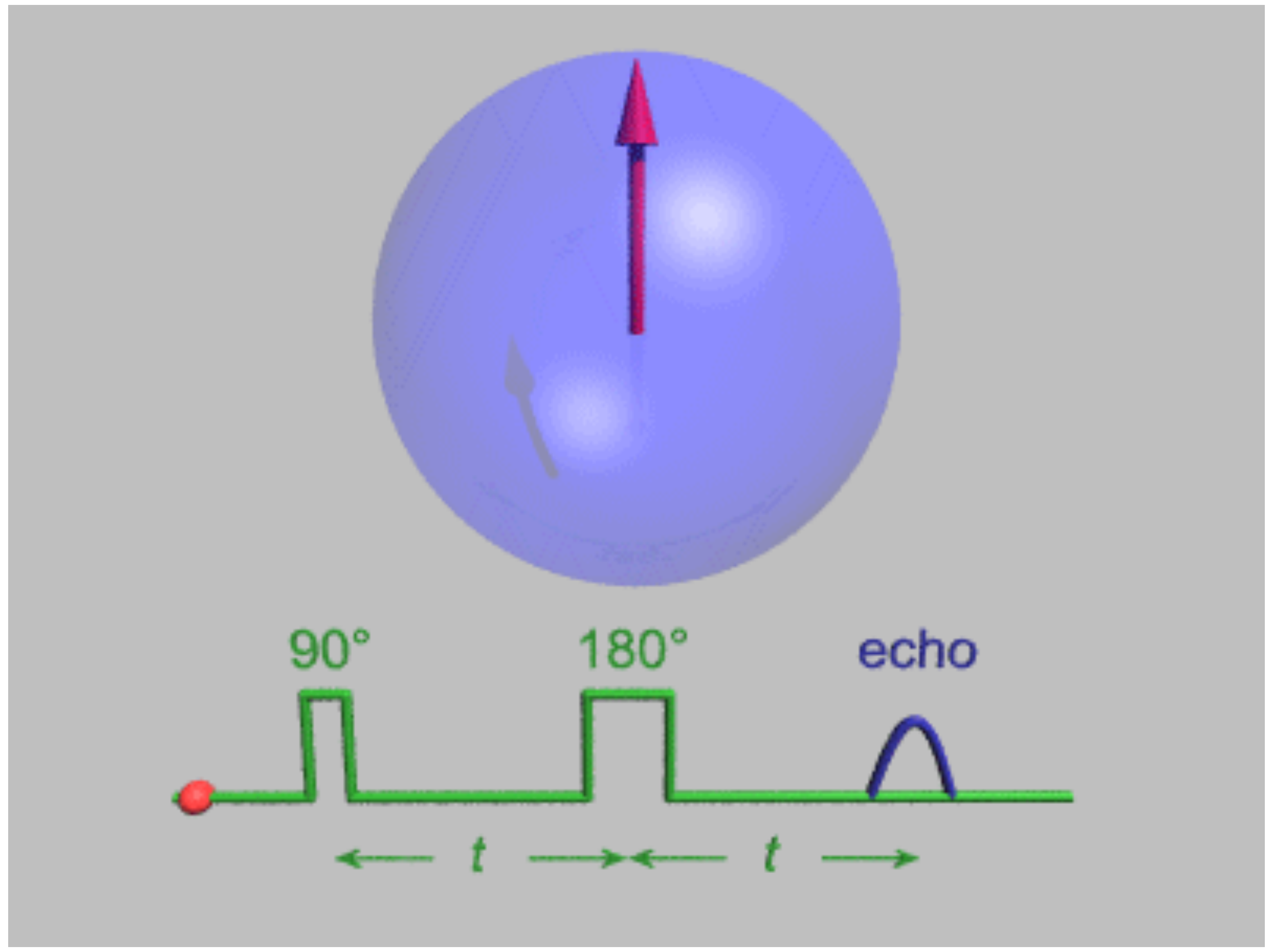

- No dephasing from inhomogeneous DC fields
- Relaxation time $T_2 \sim 50\,\mu s \gg T_2^* \sim 1\,\mu s$
- Optimized choice $\tau \sim T_2/2$

- Any DC effect cancels out from $\varphi(t)$

Sensitivity on axion DM

- Peak position

  $$\frac{m}{2\pi} \sim \frac{1}{\tau} \sim 20\,\mathrm{kHz}$$

  - Better sensitivity around the peak than DC thanks to $T_2 \gg T_2^*$

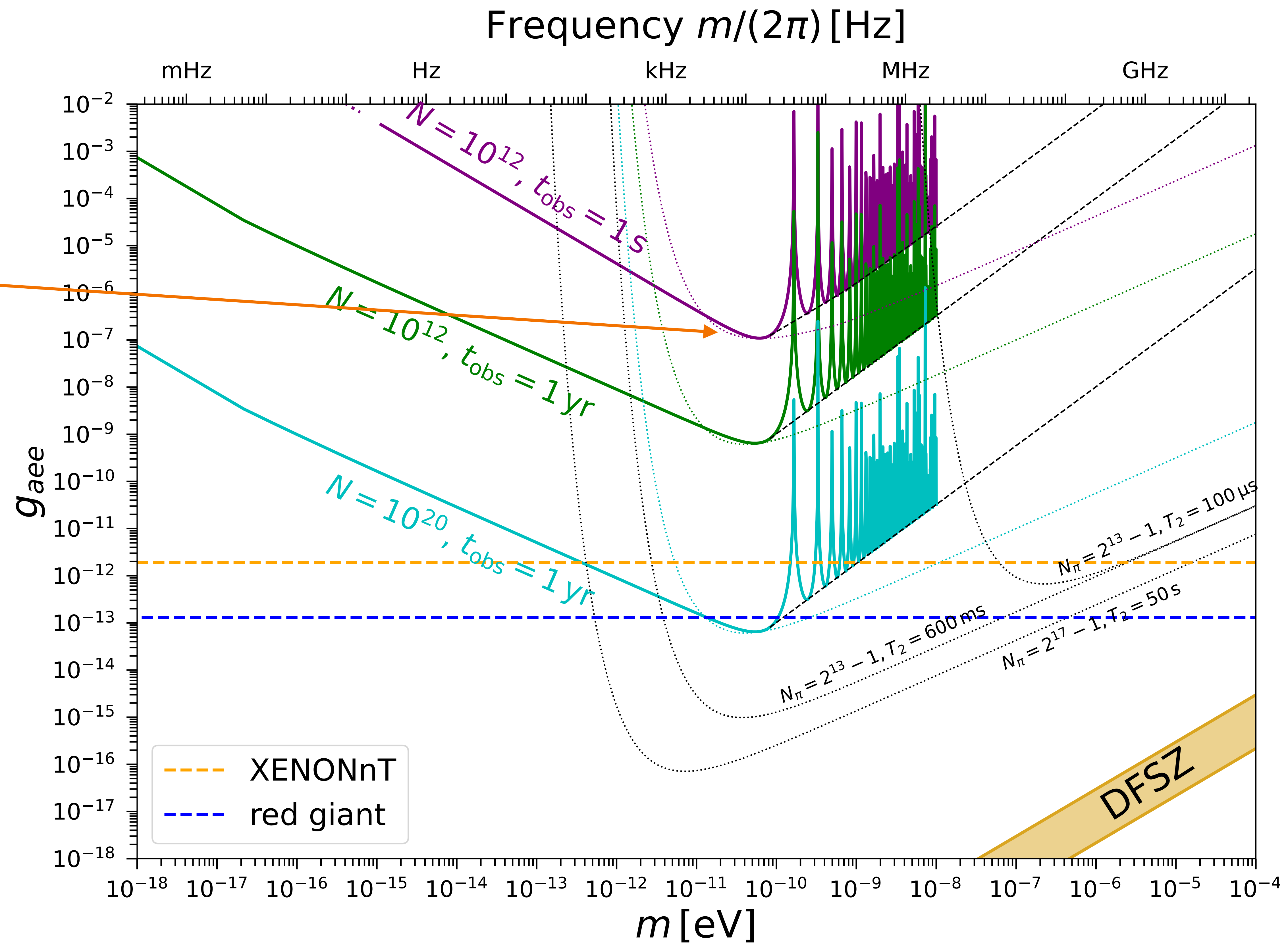

- Tunable peak position with shorter τ

Towards sensitivity improvement

- Using More π_y pulses prolongs T_2
  - Upper limit on $T_2 < T_1$
  - target frequency $\times N_\pi$

- Lower temperature prolongs T_2, T_1

  (With $N_\pi = 1023$)
  - $300\,\mathrm{K} : T_2 = 100\,\mu\mathrm{s}, T_1 \sim 1\,\mathrm{ms}$
  - $77\,\mathrm{K} : T_2 = 1\,\mathrm{ms}, T_1 \sim 1\,\mathrm{s}$
  - $4\,\mathrm{K} : T_2 = 10\,\mathrm{ms}, T_1 \gg 1\,\mathrm{s}$
  - $0.1\,\mathrm{K} : T_2 = 0.1\,\mathrm{s}, T_1 \gg 1\,\mathrm{s}$

D. Herbschleb, private communication

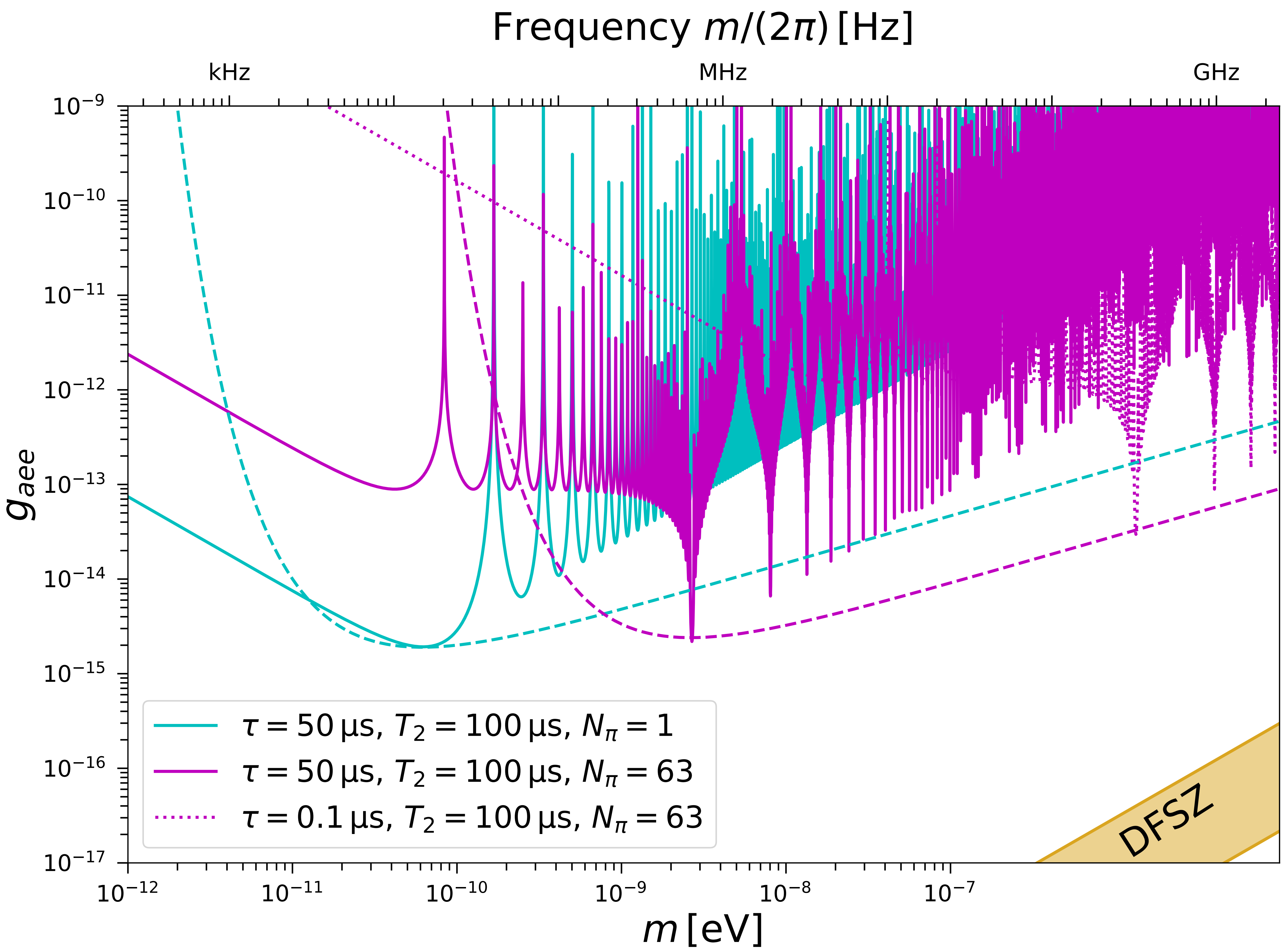

Dark photons

Shielding effect

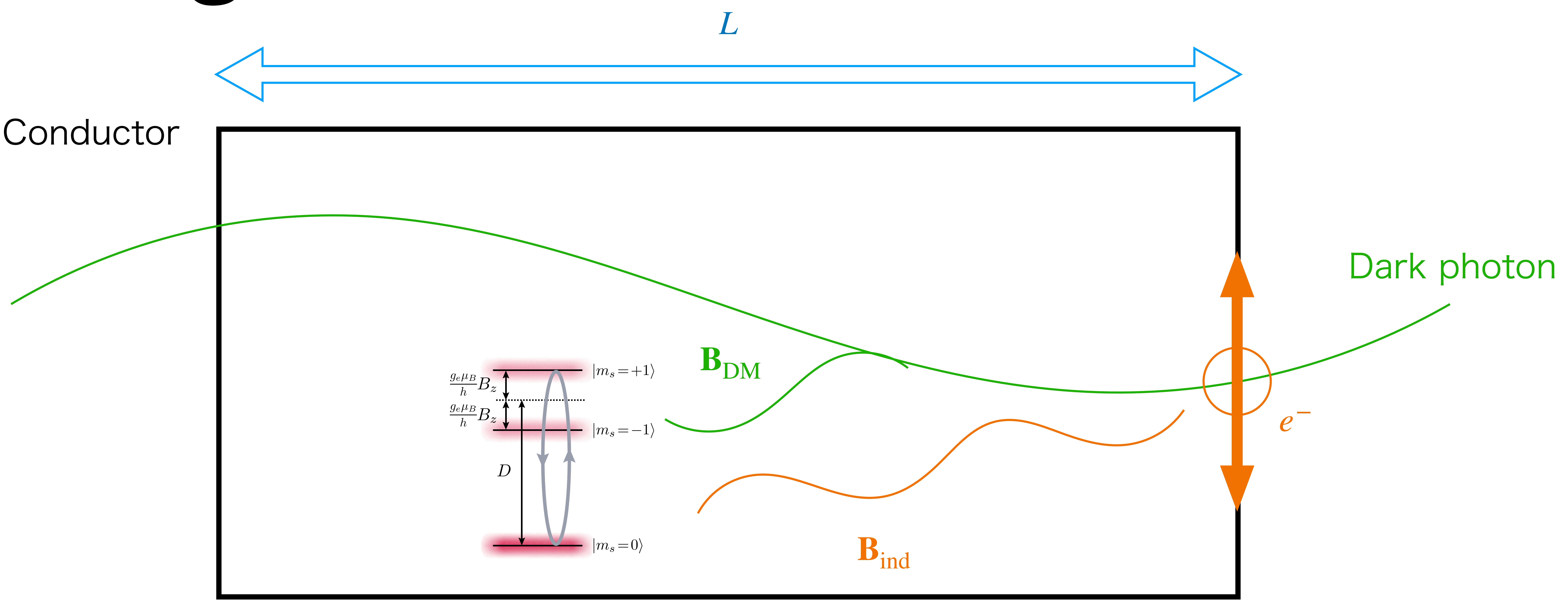

- Electric interaction of the dark photon creates current in the conductor and induces a magnetic field $\mathbf{B}_{\rm ind}$
- The effective magnetic field may be canceled and "shielded" if $\lambda_{\rm DM} > L$

S. Chaudhuri+ [1411.7382] "DM Radio" paper

NV center works without shielding

- AC magnetometry is insensitive to DC(-like) noises
  - Applicable for $\frac{m}{2\pi} \gtrsim 1\,\mathrm{kHz}$
- "Low-frequency quantum sensing" possible with Fourier analysis
  - Applicable for $\frac{m}{2\pi} \gtrsim \frac{1}{t_{\rm obs}}$

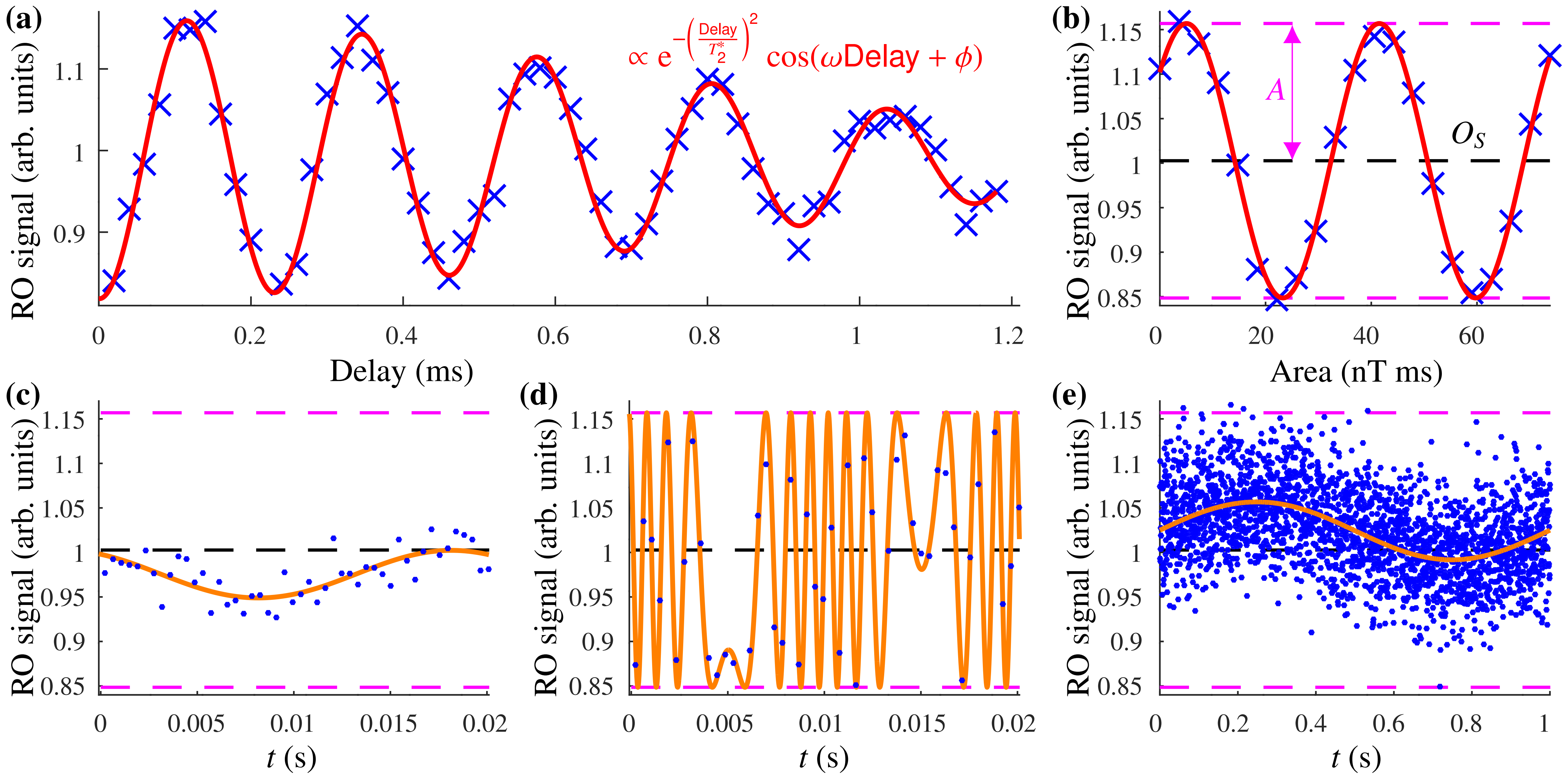

D. Herbschleb+ [2209.13870]

- Must be careful with AC magnetic noises with the target frequency

Sensitivities on dark photon DM

- DC magnetometry

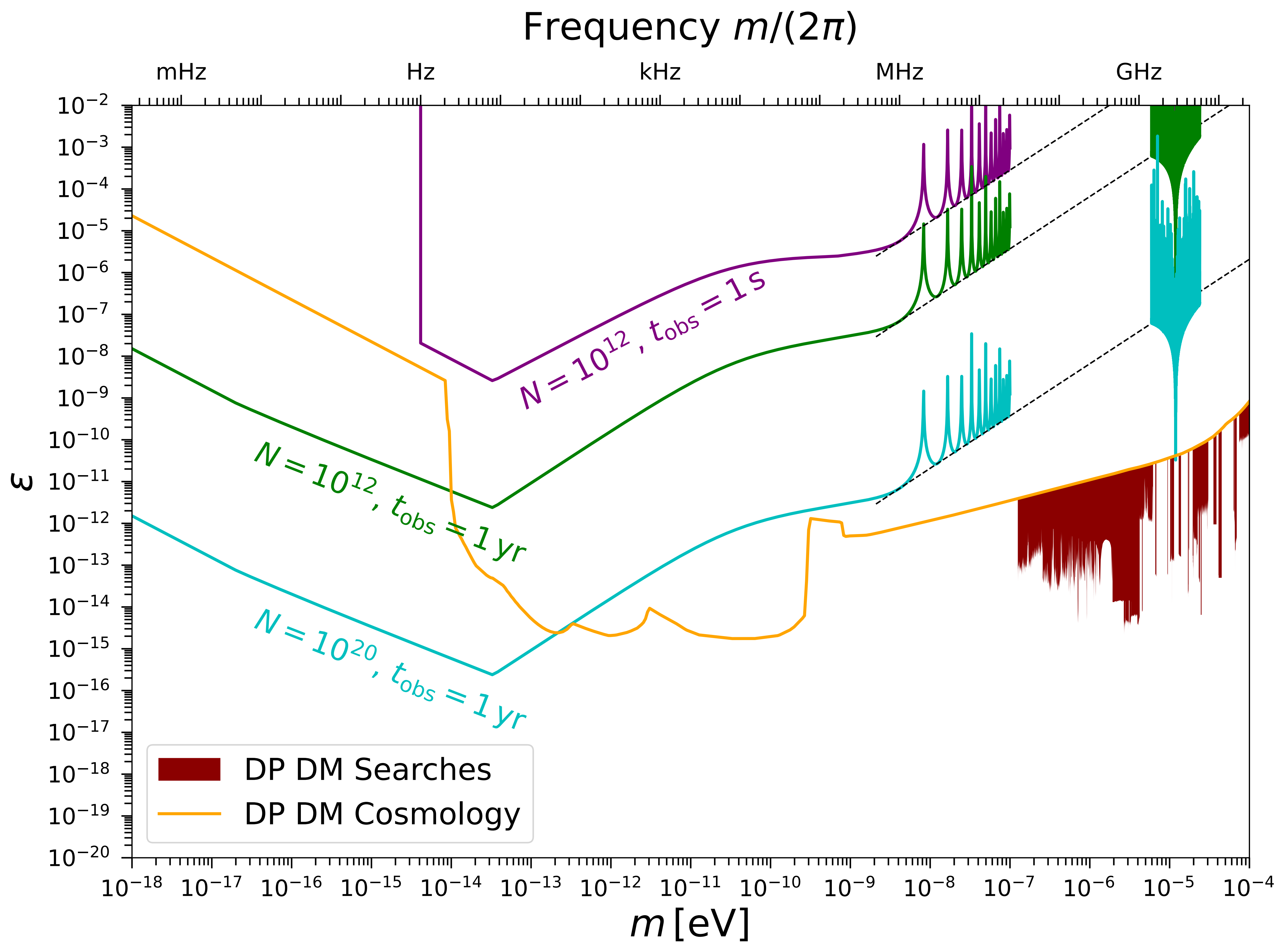

- AC magnetometry

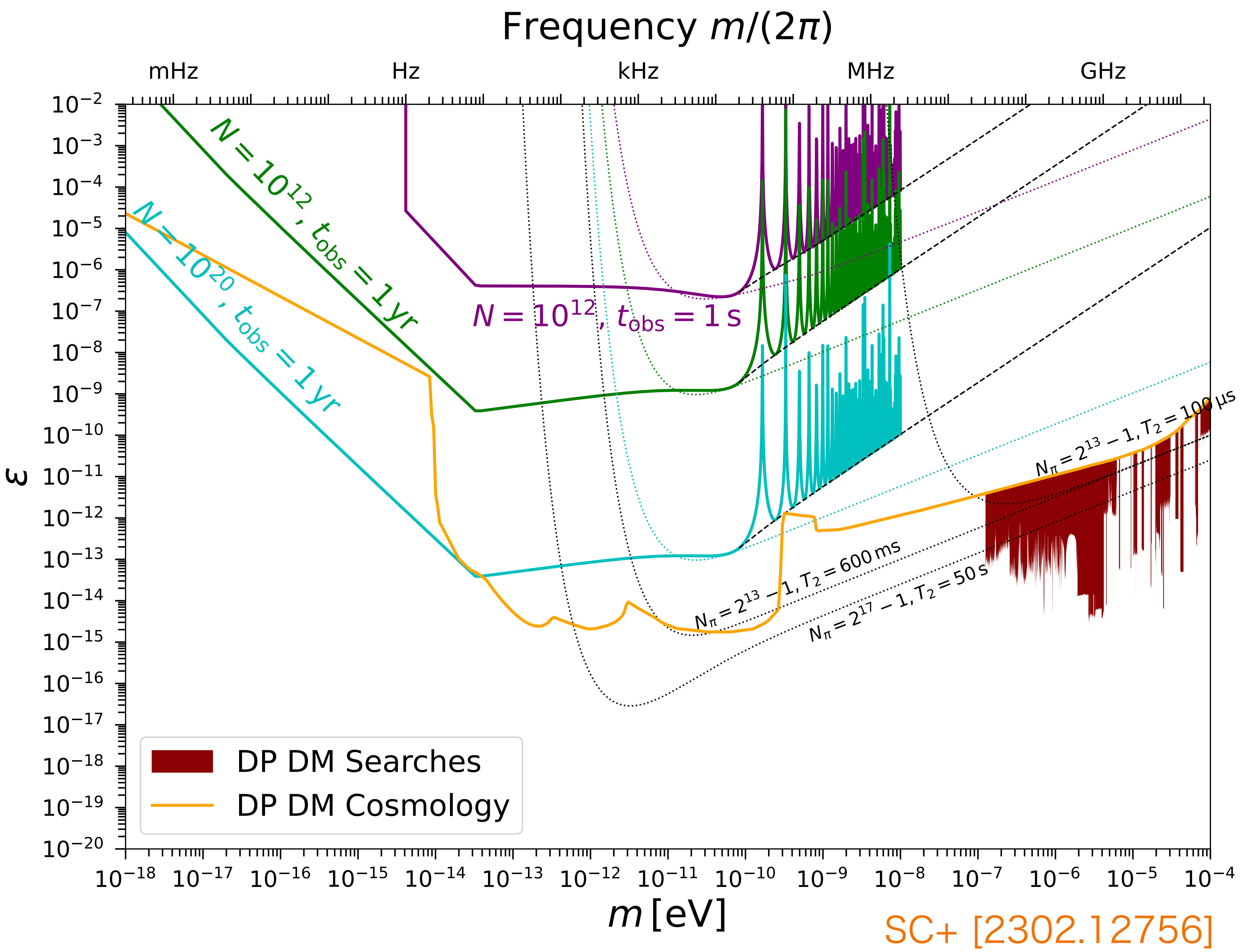

SC+ [2302.12756]

Assumptions on magnetic shielding

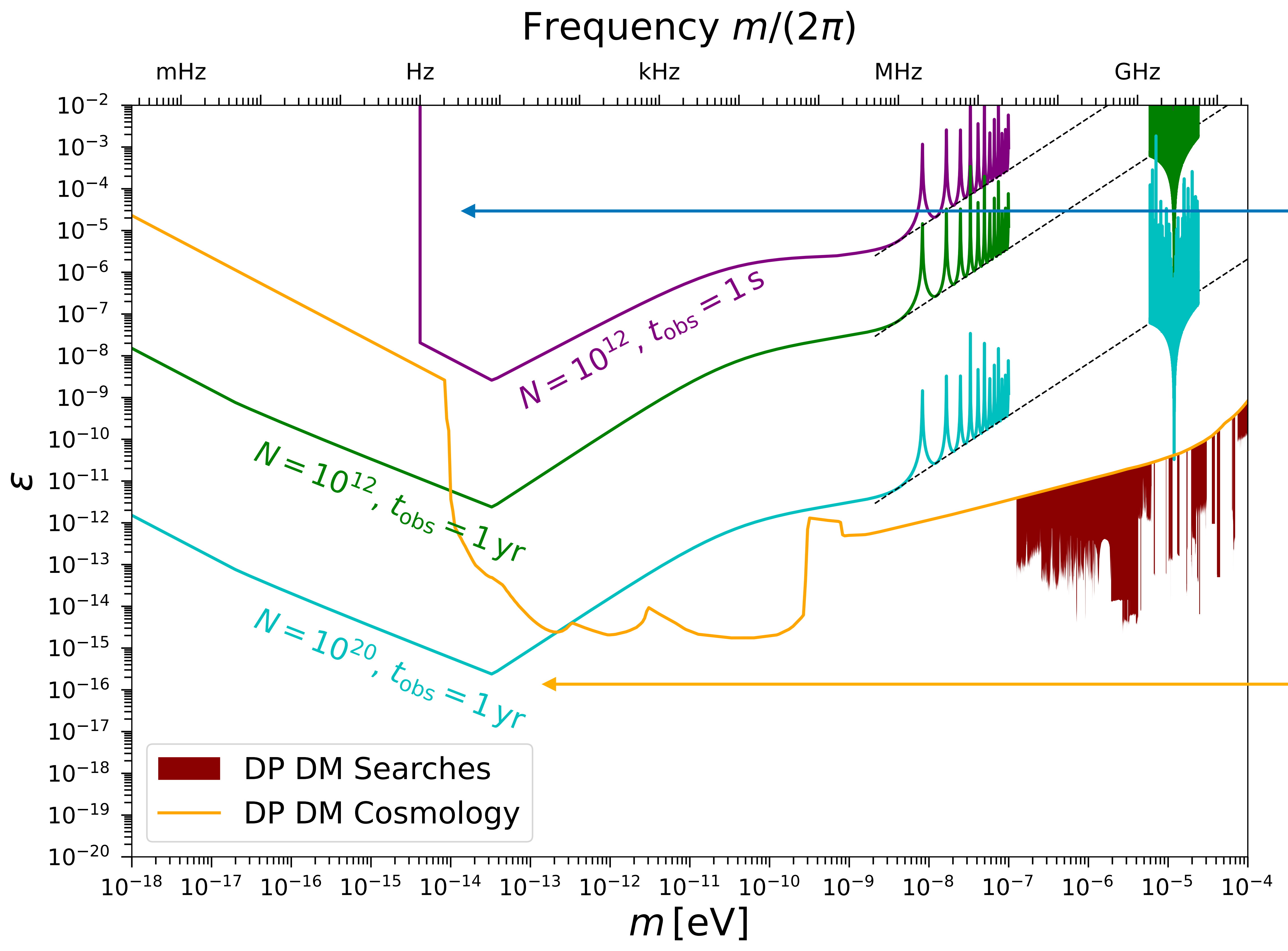

- We put shielding for $\frac{m}{2\pi} \lesssim \frac{1}{t_{obs}}$
  - Sensitivity is significantly suppressed
- Even without magnetic shielding, the inner core of the Earth/ionosphere are conducting and shielding fields
  - M. A. Fedderke+ [2106.00022]
  - Suppression factor $\propto mR_{\rm Earth}$

Experimental status

Standard-deviation quantum sensing

- Working on experimental validation of our statistical treatment

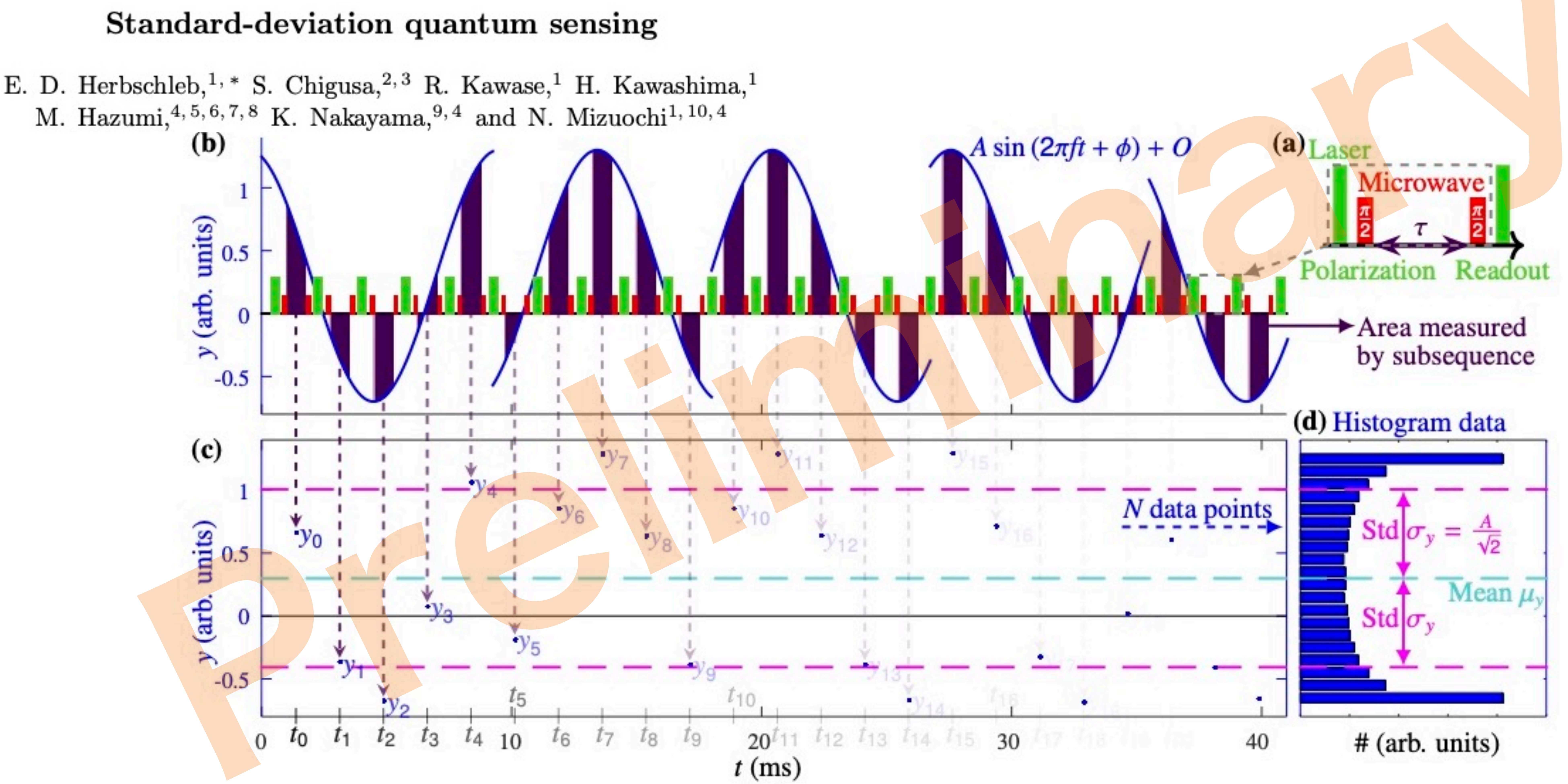

Standard-deviation quantum sensing

- Obtained expected dependence on # of data points N
- Can estimate signal amplitude and frequency

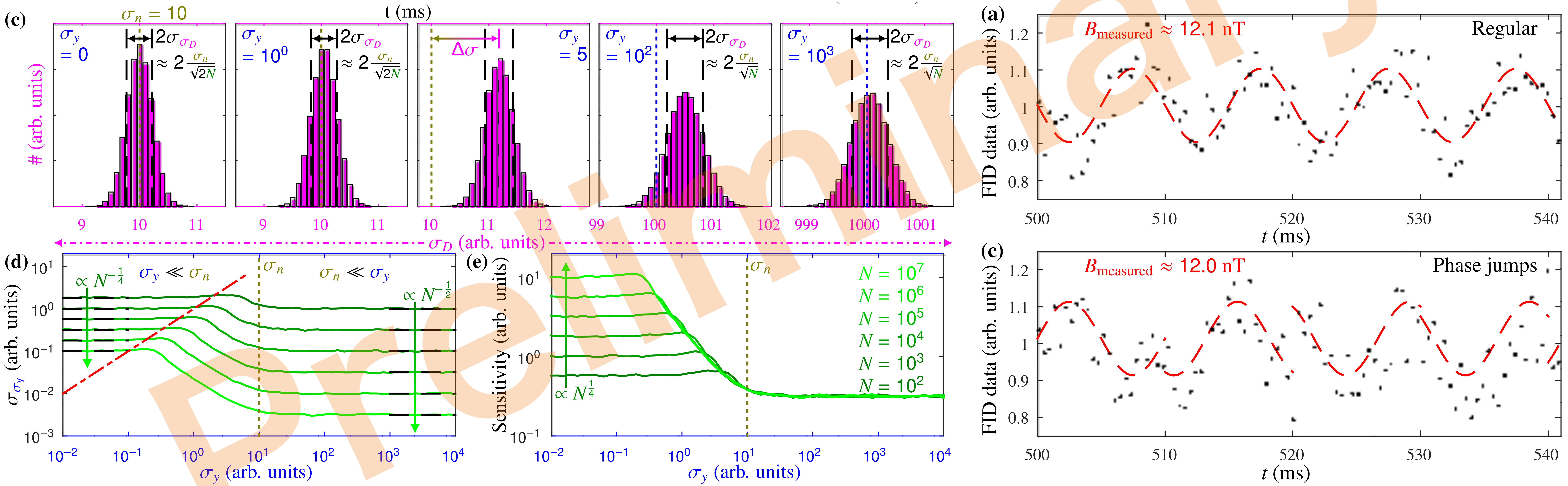

Discussions and conclusions

- We explored the potential of NV center magnetometry for DM search

- Benefits of this approach include:
  - Wide dynamic range = broad DM mass range is searched for
  - Not always need magnetic shielding

- Some applications of advanced quantum sensing techniques can be considered
  - e.g.) Use of entanglement   C. L. Degan+ “Quantum sensing”

$$|\psi\rangle = \otimes_c \frac{1}{\sqrt{2}}(|0\rangle_c + e^{i\varphi}|1\rangle_c) \quad \rightarrow \quad |\psi\rangle = \frac{1}{\sqrt{2}}(|000\ldots\rangle + e^{iN\varphi}|111\ldots\rangle)$$

International Center for
Quantum-field Measurement Systems for
Studies of the Universe and Particles
WPI research center at KEK

- Now setting up an experimental environment at QUP with NV + cryogenic

Backup slides

Sensitivity estimation

- The outcome of the spin-projection noise

$$|x\rangle \equiv \frac{1}{\sqrt{2}}\left(|0\rangle + |+\rangle\right)$$

$$\Delta S \equiv \frac{1}{2}\left[\langle x|\sigma_z^2|x\rangle - \left(\langle x|\sigma_z|x\rangle\right)^2\right]^{1/2} = \frac{1}{2}$$

- Noise contribution is $\Delta S_{\rm sp} \sim \begin{cases} \frac{1}{2}\frac{1}{\sqrt{N(t_{\rm obs}/\tau)}} & (t_{\rm obs} < \tau_a) \\ \frac{1}{2}\frac{1}{\sqrt{N(\tau_a/\tau)}}\frac{1}{\left(t_{\rm obs}/\tau_a\right)^{1/4}} & (t_{\rm obs} > \tau_a) \end{cases}$

- Sensitivity curve is $({\rm SNR}) \equiv \frac{S}{\Delta S_{\rm sp}} = 1$

Sensitivity estimation

- The axion-induced effective magnetic field has an unknown velocity $\mathbf{v}_{\rm DM}$ and phase δ

$$\mathbf{B}_{\rm DM} \simeq \sqrt{2\rho_{\rm DM}}\frac{g_{aee}}{e}\mathbf{v}_{\rm DM}\sin(m_{\rm DM}t + \delta)$$

Random velocity $\mathbf{v}_{\rm DM}$

- The signal is proportional to $\left(v_{\rm DM}^i\right)^2$ $(i = x, y, z)$, which is averaged to $\sim \frac{1}{3}v_{\rm DM}^2$

Random phase $\delta \in [0,2\pi)$

- The signal is estimated as a function of δ : $S(\delta) \propto \cos\left(\frac{m\tau}{2} + \delta\right)$

- We obtain the average $\langle S\rangle_\delta = 0$ and the standard deviation $\sqrt{\langle S^2\rangle} \neq 0$, which should be compared with the noise

Technical noise mitigation

II. MAGNETOMETRY METHOD

In many high-sensitivity measurements, technical noise such as $1/f$ noise is mitigated by moving the sensing bandwidth away from dc via upmodulation. One method, common in NV-diamond magnetometry experiments, applies frequency [12,32,41,42] or phase modulation [19,43–45] to the MWs addressing a spin transition, which causes the magnetic-field information to be encoded in a band around the modulation frequency. Here we demonstrate a multiplexed [46–49] extension of this scheme, where information from multiple NV orientations is encoded in separate frequency bands and measured on a single optical detector. Lock-in demodulation and filtering then extracts the signal associated with each NV orientation, enabling concurrent measurement of all components of a dynamic magnetic field.

J. M. Schloss+ '18